PROCEEDINGS A

royalsocietypublishing.org/journal/rspa

Research

Cite this article: Rakshit S, Bera BK, Kurths J, Ghosh D. 2019 Enhancing synchrony in multiplex network due to rewiring frequency. *Proc. R. Soc. A* **475**: 20190460. http://dx.doi.org/10.1098/rspa.2019.0460

Received: 25 July 2019
Accepted: 28 August 2019

Subject Areas:
statistical physics, complexity

Keywords:
temporal network, multiplex network, intralayer synchrony, master stability function

Author for correspondence:
Dibakar Ghosh
e-mail: dibakar@isical.ac.in

Electronic supplementary material is available online at http://dx.doi.org/10.6084/m9.figshare.c.4660811.

THE ROYAL SOCIETY PUBLISHING

Enhancing synchrony in multiplex network due to rewiring frequency

Sarbendu Rakshit[1], Bidesh K. Bera[2], Jürgen Kurths[3] and Dibakar Ghosh[1]

[1]Physics and Applied Mathematics Unit, Indian Statistical Institute, 203 B. T. Road, Kolkata 700108, India
[2]Department of Mathematics, Indian Institute of Technology Ropar, Punjab 140001, India
[3]Potsdam Institute for Climate Impact Research, Potsdam 14473, Germany

DG, 0000-0003-4832-5210

Most of the previous studies on synchrony in multiplex networks have been investigated using different types of intralayer network architectures which are either static or temporal. Effect of a temporal layer on intralayer synchrony in a multilayered network still remains elusive. In this paper, we discuss intralayer synchrony in a multiplex network consisting of static and temporal layers and how a temporal layer influences other static layers to enhance synchrony simultaneously. We analytically derive local stability conditions for intralayer synchrony based on the master stability function approach. The analytically derived results are illustrated by numerical simulations on up to five-layers multiplex networks with the paradigmatic Lorenz system as the node dynamics in each individual layer.

1. Introduction

Complex network theory offers a fertile ground to understand the intrinsic properties as well as the different emergent collective behaviours in interacting dynamical systems. In the last two decades, the network science has gained immense attention for its usefulness on the modelling of various physical, biological, social and engineering systems [1] which are widely spread in nature and society. For the natural performance, each individual unit of the networks may

© 2019 The Author(s) Published by the Royal Society. All rights reserved.

interact with other classes of networks by various ways depending on their coupling mechanism and the different types of interacting patterns which lead to the emergence of various collective phenomena. Recent research has revealed a multilayered network structure [2,3] which captures structural properties of various real-world systems in a single network architecture and gives a realistic description of naturally occurring large classes of interacting complex systems. A special case of a multilayer network is a multiplex network, where each layer is composed of the same number of nodes which interact through intralayer links and a given node on a layer be adjacent to its counter part node in the rest of the layers through interlayer links. Multiplex network basically used to encrypt highly complicated structures among interacting complex systems. In multiplex communication networks, each individual represents a physical node and the layer signifies different communication media. Using multiplex networks, different types of social relationship can be described, in which various types of social relationships yield different layers [4]. The layer communities in multiplex networks have been studied based on pairwise similarities of connection patterns between the layers [5].

Since most of the networks are supported with some internal dynamical processes, the study of the combined effect of the network's structure and the dynamical property has great importance in several disciplines. The influence of these two different properties in dynamical networks lead to the discovery of various interesting collective phenomena [6,7]. Among them, one pioneering explorations are synchronization properties [8,9] of coupled network and these phenomena have been mostly studied in the last few decades for its immense applicability in various physical [10] and engineered systems [11]. Previously, different types of synchrony properties have been studied in multiplex network organization such as cluster synchronization [12], interlayer synchronization [13,14], intralayer synchronization [15–17], the coexistence of synchrony and asynchrony [18–20], and explosive synchronization [21]. But in most cases, the network structures are considered as static networks which means that the underlying connections are invariant with respect to time. However, in real-world situations, the interactional arrangements are often not static in time. Rather, they are time varying in nature which means that the connections between the nodes created, terminated, or switched at different timescales [22]. In association with the nodal dynamical property in the network, multiplex networks strongly influence various dynamical processes and the outcome results are significantly different to the monolayer cases.

Recent research has been focused on the synchronization phenomena in the time-varying monolayer and multiplex networks. Most of the existing studies on synchrony in multiplex networks have concentrated on either all layers are static or all are time varying. The influences of coexistence of time-varying and static layers have been not explored yet, from the best of our knowledge. Previously, Stilwell *et al.* [23] studied the synchronization in a time-varying network by using the fast-switching stability criterion. The neuronal synchrony in time-varying neuronal hypernetworks has presented in [24]. Synchronization in temporal network using threshold control approach [25] and mobility of agents [26] has also been studied. But all these studies have been restricted on monolayer temporal networks. Here, we study the intralayer synchrony phenomenon in the multiplex network composed of both static and temporal layers. Particularly, here we systematically investigate the intralayer synchrony phenomenon in multiplex networks under the influence of one time-varying layer. First, we analytically prove the invariance and simultaneous occurrence of intralayer synchrony in the proposed multiplex network. Then using the master stability function (MSF) approach, we analytically derive necessary and sufficient criteria for the existence of intralayer synchrony in multiplex networks. Through the first switching criterion, the local stability of intralayer synchronization in time-varying multiplex networks investigated in terms of the time-averaged systems. Then the obtained theoretical results are illustrated by numerical experiments on up-to five-layers multiplex networks. We mainly find that the presence of rewiring frequency in the time-varying layer enhances the intralayer synchrony in the entire multiplex network. The enhancing synchrony is previously studied in coupled system using dynamic relaying [27], induced heterogeneity [28] and time-delay coupling function [29].

2. Mathematical model of a multiplex network

We consider a dynamical multiplex network consisting of single time-varying layer with M_1 and M_2 numbers of static layers above and below the time-varying layer, respectively. Each layer is composed of N number of nodes of d-dimensional dynamical systems. Its schematic diagram is depicted in figure 1. The orange and green colour layers represent the static and time-varying layers, respectively. Each black circle represent the dynamical nodes and the corresponding black lines denote the interlayer connection between the layers. The blue and red lines, respectively, represent the intralayer connections of the static and temporal layers. For particular, two time instants at $t = t_1$ and $t = t_2$, the changes of the intralayer links only in the middle layer (i.e. $l = 3$) are shown in figure 1*a*,*b*, respectively. The states of the ith node in layer-l are represented by the vectors $\mathbf{x}_{l,i}$, which are specified by a d-dimensional state variable, i.e. $\mathbf{x}_{l,i} = (x_{l,i,1}, x_{l,i,2}, \ldots, x_{l,i,d})$. Then, the dynamics of the entire multiplex network can be described as

$$\left.\begin{aligned}
\dot{\mathbf{x}}_{1,i} &= F(\mathbf{x}_{1,i}) + \epsilon \sum_{j=1}^{N} \mathscr{A}_{ij}^{[1]}\, H(\mathbf{x}_{1,j} - \mathbf{x}_{1,i}) + \eta\, G(\mathbf{x}_{2,i} - \mathbf{x}_{1,i}),\\
\dot{\mathbf{x}}_{l,i} &= F(\mathbf{x}_{l,i}) + \epsilon \sum_{j=1}^{N} \mathscr{A}_{ij}^{[l]}\, H(\mathbf{x}_{l,j} - \mathbf{x}_{l,i}) + \eta \left[G(\mathbf{x}_{l-1,i} - \mathbf{x}_{l,i}) + G(\mathbf{x}_{l+1,i} - \mathbf{x}_{l,i})\right],\\
& \qquad l = 2, 3, \ldots, M_1,\\
\dot{\mathbf{x}}_{M_1+1,i} &= F(\mathbf{x}_{M_1+1,i}) + \epsilon \sum_{j=1}^{N} \mathscr{A}_{ij}^{[M_1+1]}(t) H(\mathbf{x}_{M_1+1,j} - \mathbf{x}_{M_1+1,i})\\
&\quad + \eta\big[G(\mathbf{x}_{M_1,i} - \mathbf{x}_{M_1+1,i}) + G(\mathbf{x}_{M_1+2,i} - \mathbf{x}_{M_1+1,i})\big],\\
\dot{\mathbf{x}}_{k,i} &= F(\mathbf{x}_{k,i}) + \epsilon \sum_{j=1}^{N} \mathscr{A}_{ij}^{[k]} H(\mathbf{x}_{k,j} - \mathbf{x}_{k,i}) + \eta \left[G(\mathbf{x}_{k-1,i} - \mathbf{x}_{k,i}) + G(\mathbf{x}_{k+1,i} - \mathbf{x}_{k,i})\right],\\
& \qquad k = M_1 + 2, M_1 + 3, \ldots, M_1 + M_2\\
\text{and} \qquad \dot{\mathbf{x}}_{M_1+M_2+1,i} &= F(\mathbf{x}_{M_1+M_2+1,i}) + \epsilon \sum_{j=1}^{N} \mathscr{A}_{ij}^{[M_1+M_2+1]}\, H(\mathbf{x}_{M_1+M_2+1,j} - \mathbf{x}_{M_1+M_2+1,i})\\
&\quad + \eta G(\mathbf{x}_{M_1+M_2,i} - \mathbf{x}_{M_1+M_2+1,i}),
\end{aligned}\right\} \tag{2.1}$$

where the function $F : \mathbb{R}^d \to \mathbb{R}^d$ describes the autonomous evolution of the isolated node and the diffusion-like interaction between the layers are described by $G : \mathbb{R}^d \to \mathbb{R}^d$. Here, $H : \mathbb{R}^d \to \mathbb{R}^d$ is the vector field of the output vectors function within the layers with interaction akin to diffusion. The parameters ϵ and η are the intralayer and interlayer coupling strengths, respectively. The individual evolution function F, the intralayer coupling function H and the interlayer coupling function G are continuously differentiable with respect to their arguments with $H(0) = 0$ and $G(0) = 0$. For simplicity, here we assume that the intermediate layers are connected to its nearest layer in both sides. While the top and bottom layers are connected to its nearest one layer.

The intralayer connection of the $(M_1 + 1)$th layer is the only time-varying one, encoded by the adjacency matrix $\mathscr{A}^{[M_1+1]}(t)$, which changes with respect to time. At time t, $\mathscr{A}_{ij}^{[M_1+1]}(t) = 1$ if the ith and jth nodes are connected, and 0 otherwise. Let $\mathscr{L}^{[M_1+1]}(t)$ be the corresponding zero-row sum Laplacian matrix which reads as $\mathscr{L}_{ij}^{[M_1+1]}(t) = -\mathscr{A}_{ij}^{[M_1+1]}(t)$ for $i \neq j$, and $\mathscr{L}_{ii}^{[M_1+1]}(t) = \sum_{j=1}^{N} \mathscr{A}_{ij}^{[M_1+1]}(t)$. With the characteristic rewiring probability p_r, the links in the $(M_1 + 1)$th-layer vary over time by rewiring of each link in the entire network stochastically and independently for each time instant. Particularly, at any time t, we rewire the layer by constructing a new network independently with probability p_r. Small p_r implies that the $(M_1 + 1)$th layer is almost static as

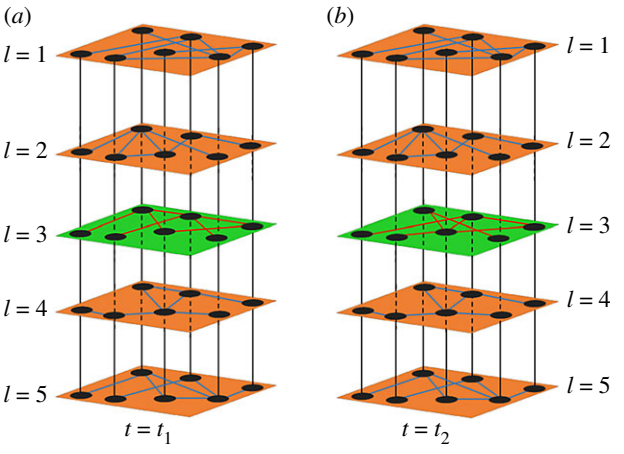

Figure 1. Schematic diagram of the proposed multiplex network of five layers ($M_1 = M_2 = 2$). Orange and green coloured layers denote the static and time-varying layers, respectively. Each black circle represents the dynamical node of the multiplex network. The solid black lines represent the interlayer links among the layers. Variation of intralayer connections (red line) only in central layer ($l = 3$) at time (*a*) $t = t_1$ and (*b*) $t = t_2$. (Online version in colour.)

the links have a very low probability of change, whereas large p_r indicates very fast switching of links implying that the network changes rapidly. While all the other intralayer connections (i.e. for the layers $l \neq M_1 + 1$) are constant over time. The interlayer connections between the layers are also static. The adjacency matrix $\mathscr{A}^{[l]}$ ($\mathscr{A}^{[l]}_{ij} = 1$ if the ith node is connected to the jth node, and 0 otherwise) describes the interaction structure of the static intralayer network configurations for layer-l ($l \neq M_1 + 1$). Its Laplacian matrix is denoted by $\mathscr{L}^{[l]}$ and defined as $\mathscr{L}^{[l]}_{ij} = -\mathscr{A}^{[l]}_{ij}$ for $i \neq j$ and $\mathscr{L}^{[l]}_{ii} = \sum_{j=1}^{N} \mathscr{A}^{[l]}_{ij}$. The diagonal matrix $\Lambda^{[l]} = \mathrm{diag}\{0 = \gamma^{[l]}_1, \gamma^{[l]}_2, \ldots, \gamma^{[l]}_N\}$ consists of the eigenvalues of $\mathscr{L}^{[l]}$.

(a) Invariance of the intralayer synchronization state

At first, we prove that for our proposed multiplex network architecture, the intralayer synchronization state is an invariant state. For this purpose, let the initial conditions of each node in a particular layer be the same, i.e. for the layer-l, each node in this layer, the initial conditions are $\mathbf{x}_{l,i}(t_0) = \mathbf{x}_l(t_0)$, for all $i = 1, 2, \ldots, N$ and $l = 1, 2, \ldots, M_1 + M_2 + 1$. Then, for the node i, the rate of change becomes

$$\left.\begin{aligned} &\dot{\mathbf{x}}_{1,i}(t_0) = F(\mathbf{x}_1(t_0)) + \eta G(\mathbf{x}_2(t_0) - \mathbf{x}_1(t_0)), \\ &\dot{\mathbf{x}}_{l,i}(t_0) = F(\mathbf{x}_l(t_0)) + \eta\big[G(\mathbf{x}_{l-1}(t_0) - \mathbf{x}_l(t_0)) + G(\mathbf{x}_{l+1}(t_0) - \mathbf{x}_l(t_0))\big], \quad l = 2, 3, \ldots, M_1 + M_2 \\ \text{and} \quad &\dot{\mathbf{x}}_{M_1+M_2+1,i}(t_0) = F(\mathbf{x}_{M_1+M_2+1}(t_0)) + \eta G(\mathbf{x}_{M_1+M_2}(t_0) - \mathbf{x}_{M_1+M_2+1}(t_0)). \end{aligned}\right\} \tag{2.2}$$

Above equations imply that $\dot{\mathbf{x}}_{l,1}(t_0) = \dot{\mathbf{x}}_{l,2}(t_0) = \cdots = \dot{\mathbf{x}}_{l,N}(t_0)$ for all $l = 1, 2, \ldots, M_1 + M_2 + 1$.

Therefore, we observe that if the layer-wise initial conditions of each node are same then their state variables will remain the same in the next time step. Proceeding with this argument for our interested time interval, we can argue that if the layer-wise initial conditions are the same then their state vectors remain the same for all course of time. This yields that the intralayer synchronization manifold is an invariant manifold.

So due to the diffusive nature of the intralayer coupling function, if all oscillators in each individual layer start with the same initial condition, then the velocity profile of all subsystems in each individual layer becomes identical. This ensures that the complete intralayer

synchronization state is an invariant state. We call the subset

$$\mathcal{S} = \{(\mathbf{x}_1^0, \mathbf{x}_2^0, \ldots, \mathbf{x}_{M_1+M_2+1}^0) \subset \mathbb{R}^{d(M_1+M_2+1)} : \mathbf{x}_{l,i} = \mathbf{x}_l^0, \text{ for } i = 1, 2, \ldots, N \text{ and } l = 1, 2, \ldots, M_1 + M_2 + 1\}, \tag{2.3}$$

as the synchronization manifold. The local stability of $\mathcal{S}$ can be determined by the intra- and interlayer coupling strengths and the spectral properties of the intralayer Laplacian matrices.

(b) Simultaneous occurrence of synchrony in each layer

In this subsection, we explore how the complete synchronization in each layer occurs together. More precisely, if the interlayer coupling strength $\eta \neq 0$ then for a particular value of the intralayer interaction strength ϵ, all the layers will be either in a synchronized or a desynchronized state. Therefore, we check by gradually increasing the value of ϵ, the complete synchrony in all the layers occur simultaneously or not, when all the layers are coupled ($\eta \neq 0$). Intralayer synchrony is another synonym of complete synchronization in each layer in a multiplex network. So to understand the mechanism of intralayer synchronization in a multiplex network, the knowledge on whether synchrony occurs simultaneously in each layer or not is essential. We prove our desired result in terms of the invariance solution of the intralayer synchronization state.

First, we consider that for a particular value of intralayer and interlayer coupling strengths ϵ and η, all the layers are in complete synchronization state at time t except one layer, say layer-k. Therefore, $\mathbf{x}_{l,1} = \mathbf{x}_{l,2} = \cdots = \mathbf{x}_{l,N}$ for all $l \neq k$. Due to the desynchronized motion of layer-k, there exist at least two nodes i_1 and i_2 in layer-k such that

$$\mathbf{x}_{k,i_1} \neq \mathbf{x}_{k,i_2} \quad \text{and} \quad \dot{\mathbf{x}}_{k,i_1} \neq \dot{\mathbf{x}}_{k,i_2}. \tag{2.4}$$

Now in layer $(k+1)$, the velocity of the node i_1 is

$$\begin{aligned}\dot{\mathbf{x}}_{k+1,i_1} = F(\mathbf{x}_{k+1,i_1}) &+ \epsilon \sum_{j=1}^{N} \mathscr{A}_{ij}^{[k+1]} H(\mathbf{x}_{k+1,j} - \mathbf{x}_{k+1,i_1}) \\ &+ \eta\big[G(\mathbf{x}_{k,i_1} - \mathbf{x}_{k+1,i_1}) + G(\mathbf{x}_{k+2,i_1} - \mathbf{x}_{k+1,i_1})\big],\end{aligned} \tag{2.5}$$

and for node i_2, it is

$$\begin{aligned}\dot{\mathbf{x}}_{k+1,i_2} = F(\mathbf{x}_{k+1,i_2}) &+ \epsilon \sum_{j=1}^{N} \mathscr{A}_{ij}^{[k+1]} H(\mathbf{x}_{k+1,j} - \mathbf{x}_{k+1,i_2}) \\ &+ \eta\big[G(\mathbf{x}_{k,i_2} - \mathbf{x}_{k+1,i_2}) + G(\mathbf{x}_{k+2,i_2} - \mathbf{x}_{k+1,i_2})\big].\end{aligned} \tag{2.6}$$

If the nodes i_1 and i_2 in the layer-$(k+1)$ are in complete synchronization state, i.e. $\mathbf{x}_{k+1,i_1} = \mathbf{x}_{k+1,i_2}$, hence from equation (2.4), we have $G(\mathbf{x}_{k,i_1} - \mathbf{x}_{k+1,i_1}) \neq G(\mathbf{x}_{k,i_2} - \mathbf{x}_{k+1,i_2})$. All the other terms of equations (2.5) and (2.6) are equal due to the complete synchronization state in layer-$(k+1)$ at time t. Since $\eta \neq 0$, the velocities of the nodes i_1 and i_2 in the layer-$(k+1)$ become unequal at time t. These yield a separate solution trajectories of the nodes i_1 and i_2 hereafter, i.e. layer-$(k+1)$ becomes desynchronized after time t. So the desynchronized motion in the layer-k propagates in the layer-$(k+1)$.

Similarly, all the nodes in the layer-$(k-1)$ are in complete synchronization state at time t, so we have $F(\mathbf{x}_{k-1,i_1}) = F(\mathbf{x}_{k-1,i_2})$, $G(\mathbf{x}_{k-2,i_1} - \mathbf{x}_{k-1,i_1}) = G(\mathbf{x}_{k-2,i_2} - \mathbf{x}_{k-1,i_2})$ and $H(\mathbf{x}_{k-1,j} - \mathbf{x}_{k-1,i_1}) = H(\mathbf{x}_{k-1,j} - \mathbf{x}_{k-1,i_2})$ for all j. Due to the desynchronized motion of the nodes i_1 and i_2 in the layer-k, we have $G(\mathbf{x}_{k,i_1} - \mathbf{x}_{k-1,i_1}) \neq G(\mathbf{x}_{k,i_2} - \mathbf{x}_{k-1,i_2})$. So with the same value of the state variables, the velocities of the nodes i_1 and i_2 in the layer-$(k-1)$ become unequal at time t. This also gives the desynchronization motion of the nodes i_1 and i_2 hereafter in this layer.

Therefore, the desynchronization motion in the layer-k propagates in the layers-$(k+1)$ and $(k-1)$. Likewise the desynchronize motions of the layers-$(k-1), k, (k+1)$ will propagate to the layers-$(k-2)$ and $(k+2)$ within a very short time. Successively within a short time interval,

each layer in the multiplex network (2.1) becomes desynchronized due to the presence of one desynchronized layer. Thus, the desynchronized layers will never coexist with the synchronize layers, if the interlayer coupling strength $\eta \neq 0$. A desynchronized layer is sufficient to destroy the coherent motion of all the other layers. So from the above discussion, we can conclude that complete synchronization occurs in all the layers simultaneously.

Next, we devote our study on the investigation of the stability of the intralayer synchronization state in the multiplex network (2.1). By using an eigenvalue analysis in the next section, we analytically derive a stability criterion for synchrony.

3. Local stability of intralayer synchronization state

Using the MSF approach [30], in this section, we analyse the stability of the intralayer synchronization state in $(M_1 + M_2 + 1)$ layers multiplex network (2.1). In our considered multiplex network only the $(M_1 + 1)$th layer is time varying, but all the other layers are stagnant. In this paper, our aim is to investigate the effects of this temporal layer on the emergence of synchrony in the other static layers. For the stability of the intralayer synchronization state, we analyse the stability of the corresponding error dynamics which contain the transverse together with one parallel direction. By projecting the error vector onto the Laplacian eigenspace, we can separate out the parallel components, while for time-varying networks, the Laplacian eigenspace varies with the Laplacian matrix. So the transformation of the error vectors is not possible. To-get-rid from this difficulty, we use the fast switching stability criterion [23], through which for sufficiently fast switching, the temporal network can be approximated by a time-averaged network.

For sufficient fast rewiring, we can approximate our time-varying multiplex network by a time-average static network. For this, there exists a constant T such that $\mathscr{A}^{[M_1+1]} = 1/T \int_t^{t+T} \mathscr{A}^{[M_1+1]}(\tau)\,\mathrm{d}\tau, t \in \mathbb{R}$. Here the time t is arbitrarily chosen, but the time interval T (sufficiently large) depends on the individual dynamics $F(\mathbf{x})$ of each node, intralayer coupling function $H(\mathbf{x})$, interlayer coupling function $G(\mathbf{x})$ and also how fast the time-varying layer is switching. Then the corresponding time-averaged multiplex network becomes

$$\left.\begin{aligned}
\dot{\mathbf{x}}_{1,i} &= F(\mathbf{x}_{1,i}) + \epsilon \sum_{j=1}^{N} \mathscr{A}_{ij}^{[1]} H(\mathbf{x}_{1,j} - \mathbf{x}_{1,i}) + \eta G(\mathbf{x}_{2,i} - \mathbf{x}_{1,i}),\\
\dot{\mathbf{x}}_{l,i} &= F(\mathbf{x}_{l,i}) + \epsilon \sum_{j=1}^{N} \mathscr{A}_{ij}^{[l]} H(\mathbf{x}_{l,j} - \mathbf{x}_{l,i}) + \eta\big[G(\mathbf{x}_{l-1,i} - \mathbf{x}_{l,i}) + G(\mathbf{x}_{l+1,i} - \mathbf{x}_{l,i})\big],\\
& \quad l = 2, 3, \ldots, M_1,\\
\dot{\mathbf{x}}_{M_1+1,i} &= F(\mathbf{x}_{M_1+1,i}) + \epsilon \sum_{j=1}^{N} \mathscr{A}_{ij}^{[M_1+1]} H(\mathbf{x}_{M_1+1,j} - \mathbf{x}_{M_1+1,i}) + \eta\big[G(\mathbf{x}_{M_1,i} - \mathbf{x}_{M_1+1,i})\\
& \quad + G(\mathbf{x}_{M_1+2,i} - \mathbf{x}_{M_1+1,i})\big],\\
\dot{\mathbf{x}}_{k,i} &= F(\mathbf{x}_{k,i}) + \epsilon \sum_{j=1}^{N} \mathscr{A}_{ij}^{[k]} H(\mathbf{x}_{k,j} - \mathbf{x}_{k,i}) + \eta\big[G(\mathbf{x}_{k-1,i} - \mathbf{x}_{k,i}) + G(\mathbf{x}_{k+1,i} - \mathbf{x}_{k,i})\big],\\
& \quad k = M_1 + 2, M_1 + 3, \ldots, M_1 + M_2\\
\text{and} \quad \dot{\mathbf{x}}_{M_1+M_2+1,i} &= F(\mathbf{x}_{M_1+M_2+1,i}) + \epsilon \sum_{j=1}^{N} \mathscr{A}_{ij}^{[M_1+M_2+1]} H(\mathbf{x}_{M_1+M_2+1,j} - \mathbf{x}_{M_1+M_2+1,i})\\
& \quad + \eta G(\mathbf{x}_{M_1+M_2,i} - \mathbf{x}_{M_1+M_2+1,i}).
\end{aligned}\right\} \tag{3.1}$$

For sufficient fast switching, this time-averaged multiplex network (3.1) and the original time-varying multiplex network (2.1) gives the same synchronization transition. Denote the time-average Laplacian matrix for the layer-(M_1+1) by $\bar{\mathscr{L}}^{[M_1+1]}$. Also assume that its eigenvalues are $\{0=\bar{\gamma}_1^{[M_1+1]},\bar{\gamma}_2^{[M_1+1]},\ldots,\bar{\gamma}_N^{[M_1+1]}\}$. Also, let $\bar{\Lambda}^{[M_1+1]}$ be a diagonal matrix of eigenvalues and $\bar{V}^{[M_1+1]}$ be the corresponding matrix of eigenvectors.

At intralayer synchronization states, let each layer of this multiplex network evolves synchronously with the synchronization manifold $(\mathbf{x}_1(t),\mathbf{x}_2(t),\ldots,\mathbf{x}_{M_1+M_2+1}(t))$ obtained from the evolution equation

$$\left.\begin{aligned}\dot{\mathbf{x}}_1&=F(\mathbf{x}_1)+\eta G(\mathbf{x}_2-\mathbf{x}_1),\\ \dot{\mathbf{x}}_l&=F(\mathbf{x}_l)+\eta\big[G(\mathbf{x}_{l-1}-\mathbf{x}_l)+G(\mathbf{x}_{l+1}-\mathbf{x}_l)\big],\qquad l=2,3,\ldots,M_1+M_2\\ \text{and}\qquad \dot{\mathbf{x}}_{M_1+M_2+1}&=F(\mathbf{x}_{M_1+M_2+1})+\eta G(\mathbf{x}_{M_1+M_2}-\mathbf{x}_{M_1+M_2+1}).\end{aligned}\right\}\tag{3.2}$$

Considering small perturbation $\delta\mathbf{x}_{l,i}(t)$ of the ith node in the layer-l from its complete synchronization state. Then its state variables become $\mathbf{x}_{l,i}(t)=\mathbf{x}_l(t)+\delta\mathbf{x}_{l,i}(t)$ for $l=1,2,\ldots,M_1+M_2+1$ and $i=1,2,\ldots,N$. Then linearizing around the synchronization manifold (3.2), the error dynamics of the corresponding time-average systems can be written as

$$\left.\begin{aligned}\delta\dot{\mathbf{x}}_{1,i}&=JF(\mathbf{x}_1)\delta\mathbf{x}_{1,i}-\epsilon\sum_{j=1}^{N}\mathscr{L}_{ij}^{[1]}JH(0)\delta\mathbf{x}_{1,j}+\eta JG(\mathbf{x}_2-\mathbf{x}_1)(\delta\mathbf{x}_{2,i}-\delta\mathbf{x}_{1,i}),\\ \delta\dot{\mathbf{x}}_{l,i}&=JF(\mathbf{x}_l)\delta\mathbf{x}_{l,i}-\epsilon\sum_{j=1}^{N}\mathscr{L}_{ij}^{[l]}JH(0)\delta\mathbf{x}_{l,j}+\eta\big[JG(\mathbf{x}_{l-1}-\mathbf{x}_l)(\delta\mathbf{x}_{l-1,i}-\delta\mathbf{x}_{l,i})\\ &\quad+JG(\mathbf{x}_{l+1}-\mathbf{x}_l)(\delta\mathbf{x}_{l+1,i}-\delta\mathbf{x}_{l,i})\big],\quad l=2,3,\ldots,M_1,\\ \delta\dot{\mathbf{x}}_{M_1+1,i}&=JF(\mathbf{x}_{M_1+1})\delta\mathbf{x}_{M_1+1,i}-\epsilon\sum_{j=1}^{N}\bar{\mathscr{L}}_{ij}^{[M_1+1]}JH(0)\delta\mathbf{x}_{M_1+1,j}\\ &\quad+\eta\big[JG(\mathbf{x}_{M_1}-\mathbf{x}_{M_1+1})(\delta\mathbf{x}_{M_1,i}-\delta\mathbf{x}_{M_1+1,i})+JG(\mathbf{x}_{M_1+2}\\ &\quad-\mathbf{x}_{M_1+1})(\delta\mathbf{x}_{M_1+2,i}-\delta\mathbf{x}_{M_1+1,i})\big],\\ \delta\dot{\mathbf{x}}_{k,i}&=JF(\mathbf{x}_k)\delta\mathbf{x}_{k,i}-\epsilon\sum_{j=1}^{N}\mathscr{L}_{ij}^{[k]}JH(0)\delta\mathbf{x}_{k,i}+\eta\big[JG(\mathbf{x}_{k-1}-\mathbf{x}_k)(\delta\mathbf{x}_{k-1,i}-\delta\mathbf{x}_{k,i})\\ &\quad+JG(\mathbf{x}_{k+1}-\mathbf{x}_k)(\delta\mathbf{x}_{k+1,i}-\delta\mathbf{x}_{k,i})\big],\quad k=M_1+2,M_1+3,\ldots,M_1+M_2\\ \text{and}\qquad \delta\dot{\mathbf{x}}_{M_1+M_2+1,i}&=JF(\mathbf{x}_{M_1+M_2+1})\delta\mathbf{x}_{M_1+M_2+1,i}-\epsilon\sum_{j=1}^{N}\mathscr{L}_{ij}^{[M_1+M_2+1]}JH(0)(\delta\mathbf{x}_{M_1+M_2+1,j})\\ &\quad+\eta JG(\mathbf{x}_{M_1+M_2}-\mathbf{x}_{M_1+M_2+1})(\delta\mathbf{x}_{M_1+M_2,i}-\delta\mathbf{x}_{M_1+M_2+1,i}),\end{aligned}\right\}\tag{3.3}$$

where JF denotes the Jacobian of the function F. For each layer-l, there exist exactly $(N-1)$ independent transverse error components, which are $(\mathbf{x}_{l,2}-\mathbf{x}_{l,1}),(\mathbf{x}_{l,3}-\mathbf{x}_{l,1}),\ldots,(\mathbf{x}_{l,N}-\mathbf{x}_{l,1})$. So for the entire (M_1+M_2+1) layer multiplex network, there are exactly $(N-1)(M_1+M_2+1)$ mutually independent transverse error components. But in the above error systems, there are $N(M_1+M_2+1)$ state variables which correspond to different error vectors. Therefore, the error systems (3.3) should contain additional (M_1+M_2+1) parallel components. So the stabilization of the intralayer synchronization state does not imply a stabilization of the above error systems, unless otherwise we eliminate the parallel components. For this purpose, we project the error components $\{\delta\mathbf{x}_{l,i}:l=1,2,\ldots,M_1+M_2+1;\ i=1,2,\ldots,N\}$ onto the Laplacian eigenspace of any-one of the intralayer Laplacian matrix. Since the eigenspace of all the Laplacian matrices forms N equivalent basis of $\mathbb{R}^N$, we are free to choose any one intralayer

Laplacian matrix. Here, we choose the time-average Laplacian matrix $\bar{\mathscr{L}}^{[M_1+1]}$. For the time-averaged layer, $\bar{V}^{[M_1+1]^{-1}}\bar{\mathscr{L}}^{[M_1+1]}\bar{V}^{[M_1+1]} = \bar{\Lambda}^{[M_1+1]}$, and for the other static intralayer Laplacian matrix $V^{[l]^{-1}}\mathscr{L}^{[l]}V^{[l]} = \Lambda^{[l]}$.

For simplicity, we denote $\delta\mathbf{x}_l(t) = [\delta\mathbf{x}_{l,1}(t)^{tr}, \delta\mathbf{x}_{l,2}(t)^{tr}, \ldots, \delta\mathbf{x}_{l,N}(t)^{tr}]^{tr}$. Then the evolution of the error dynamics in vectorial form becomes

$$\left.\begin{aligned}
\delta\dot{\mathbf{x}}_1 &= [I_N \otimes JF(\mathbf{x}_1) - \epsilon\mathscr{L}^{[1]} \otimes JH(0)]\delta\mathbf{x}_1 + \eta I_N \otimes JG(\mathbf{x}_2 - \mathbf{x}_1)(\delta\mathbf{x}_2 - \delta\mathbf{x}_1),\\
\delta\dot{\mathbf{x}}_l &= [I_N \otimes JF(\mathbf{x}_l) - \epsilon\mathscr{L}^{[l]} \otimes JH(0)]\delta\mathbf{x}_l + \eta\big[I_N \otimes JG(\mathbf{x}_{l-1} - \mathbf{x}_l)(\delta\mathbf{x}_{l-1} - \delta\mathbf{x}_l)\\
&\quad + I_N \otimes JG(\mathbf{x}_{l+1} - \mathbf{x}_l)(\delta\mathbf{x}_{l+1} - \delta\mathbf{x}_l)\big], \quad l = 2, 3, \ldots, M_1,\\
\delta\dot{\mathbf{x}}_{M_1+1} &= [I_N \otimes JF(\mathbf{x}_{M_1+1}) - \epsilon\bar{\mathscr{L}}^{[M_1+1]} \otimes JH(0)]\delta\mathbf{x}_{M_1+1}\\
&\quad + \eta\big[I_N \otimes JG(\mathbf{x}_{M_1} - \mathbf{x}_{M_1+1})(\delta\mathbf{x}_{M_1} - \delta\mathbf{x}_{M_1+1})\\
&\quad + I_N \otimes JG(\mathbf{x}_{M_1+2} - \mathbf{x}_{M_1+1})(\delta\mathbf{x}_{M_1+2} - \delta\mathbf{x}_{M_1+1})\big],\\
\delta\dot{\mathbf{x}}_k &= [I_N \otimes JF(\mathbf{x}_k) - \epsilon\mathscr{L}^{[k]} \otimes JH(0)]\delta\mathbf{x}_k + \eta\big[I_N \otimes JG(\mathbf{x}_{k-1} - \mathbf{x}_k)(\delta\mathbf{x}_{k-1} - \delta\mathbf{x}_k)\\
&\quad + I_N \otimes JG(\mathbf{x}_{k+1} - \mathbf{x}_k)(\delta\mathbf{x}_{k+1} - \delta\mathbf{x}_k)\big], \quad k = M_1 + 2, M_1 + 3, \ldots, M_1 + M_2\\
\text{and}\quad \delta\dot{\mathbf{x}}_{M_1+M_2+1} &= [I_N \otimes JF(\mathbf{x}_{M_1+M_2+1}) - \epsilon\mathscr{L}^{[M_1+M_2+1]} \otimes JH(0)]\delta\mathbf{x}_{M_1+M_2+1}\\
&\quad + \eta[I_N \otimes JG(\mathbf{x}_{M_1+M_2} - \mathbf{x}_{M_1+M_2+1})](\delta\mathbf{x}_{M_1+M_2} - \delta\mathbf{x}_{M_1+M_2+1}).
\end{aligned}\right\} \tag{3.4}$$

Here, $\otimes$ is the matrix Kronecker product. Projecting the error components onto the eigenspace of $\bar{\mathscr{L}}^{[M_1+1]}$, we get the transformed error components as

$$\xi_l(t) = \left(\bar{V}^{[M_1+1]} \otimes I_d\right)^{-1}\delta\mathbf{x}_l(t), \quad l = 1, 2, \ldots, M_1 + M_2 + 1. \tag{3.5}$$

These projected components are dominated by the evolution equation

$$\left.\begin{aligned}
\dot{\xi}_1 &= [I_N \otimes JF(\mathbf{x}_1) - \epsilon\bar{V}^{[M_1+1]^{-1}}\mathscr{L}^{[1]}\bar{V}^{[M_1+1]} \otimes JH(0)]\xi_1\\
&\quad + \eta\, I_N \otimes JG(\mathbf{x}_2 - \mathbf{x}_1)(\xi_2 - \xi_1),\\
\dot{\xi}_l &= [I_N \otimes JF(\mathbf{x}_l) - \epsilon\bar{V}^{[M_1+1]^{-1}}\mathscr{L}^{[l]}\bar{V}^{[M_1+1]} \otimes JH(0)]\xi_l\\
&\quad + \eta\big[I_N \otimes JG(\mathbf{x}_{l-1} - \mathbf{x}_l)(\xi_{l-1} - \xi_l)\\
&\quad + I_N \otimes JG(\mathbf{x}_{l+1} - \mathbf{x}_l)(\xi_{l+1} - \xi_l)\big], \quad l = 2, 3, \ldots, M_1,\\
\dot{\xi}_{M_1+1} &= [I_N \otimes JF(\mathbf{x}_{M_1+1}) - \epsilon\bar{V}^{[M_1+1]^{-1}}\bar{\mathscr{L}}^{[M_1+1]}\bar{V}^{[M_1+1]} \otimes JH(0)]\xi_{M_1+1}\\
&\quad + \eta\big[I_N \otimes JG(\mathbf{x}_{M_1} - \mathbf{x}_{M_1+1})(\xi_{M_1} - \xi_{M_1+1})\\
&\quad + I_N \otimes JG(\mathbf{x}_{M_1+2} - \mathbf{x}_{M_1+1})(\xi_{M_1+2} - \xi_{M_1+1})\big],\\
\dot{\xi}_k &= [I_N \otimes JF(\mathbf{x}_k) - \epsilon\bar{V}^{[M_1+1]^{-1}}\mathscr{L}^{[k]}\bar{V}^{[M_1+1]} \otimes JH(0)]\xi_k\\
&\quad + \eta\big[I_N \otimes JG(\mathbf{x}_{k-1} - \mathbf{x}_k)(\xi_{k-1} - \xi_k) + I_N \otimes JG(\mathbf{x}_{k+1} - \mathbf{x}_k)(\xi_{k+1} - \xi_k)\big],\\
&\quad k = M_1 + 2, M_1 + 3, \ldots, M_1 + M_2\\
\text{and}\quad \dot{\xi}_{M_1+M_2+1} &= [I_N \otimes JF(\mathbf{x}_{M_1+M_2+1})\\
&\quad - \epsilon\bar{V}^{[M_1+1]^{-1}}\mathscr{L}^{[M_1+M_2+1]}\bar{V}^{[M_1+1]} \otimes JH(0)]\xi_{M_1+M_2+1}\\
&\quad + \eta[I_N \otimes JG(\mathbf{x}_{M_1+M_2} - \mathbf{x}_{M_1+M_2+1})](\xi_{M_1+M_2} - \xi_{M_1+M_2+1}).
\end{aligned}\right\} \tag{3.6}$$

Now for the layer-$(M_1 + 1)$, we can write $\bar{V}^{[M_1+1]^{-1}}\mathscr{L}^{[M_1+1]}\bar{V}^{[M_1+1]} = \bar{\Lambda}^{[M_1+1]}$, which is a diagonal matrix. For the other static layer-k ($k = 1, 2, \ldots, M_1, M_1 + 2, \ldots, M_1 + M_2 + 1$),

$$\bar{V}^{[M_1+1]^{-1}}\mathscr{L}^{[k]}\bar{V}^{[M_1+1]} = \left[V^{[k]^{-1}}\bar{V}^{[M_1+1]}\right]^{-1}\mathscr{L}^{[k]}\left[V^{[k]^{-1}}\bar{V}^{[M_1+1]}\right],$$

where $V^{[k]}$ is the orthonormal basis of eigenvectors of the Laplacian matrix $\mathscr{L}^{[k]}$. Now there is no guarantee that these static Laplacian matrices will commute with the average Laplacian matrix $\bar{V}^{[M_1+1]}$. Therefore, the intralayer coupling term of the above projected equation may not be block diagonal. Merely, the ith component of $\Gamma^{[k]^{-1}}\mathscr{L}^{[k]}\Gamma^{[k]} \otimes JH(0)\xi_k$ can be written as $\sum_{s=2}^{N}\sum_{r=2}^{N}\Gamma_{rs}^{[k]}\gamma_r^{[k]}\Gamma_{ri}^{[k]}\xi_{ks}$. In the summation, the range of the dummy index r starts from 2 because the first eigenvalue is zero corresponding to $r=1$. Similarly, the term $s=1$ can also be ignored due to the orthonormality of the Laplacian eigenvectors. All the elements of the first row and first column of $\Gamma^{[k]}$ are equal to zero, except $\Gamma_{1,1}^{[k]}=1$. Then the transverse error dynamics becomes

$$\left.\begin{aligned}
\dot{\xi}_{1,i} &= JF(\mathbf{x}_1)\xi_{1,i} - \epsilon\sum_{s=2}^{N}\sum_{r=2}^{N}\Gamma_{rs}^{[1]}\gamma_r^{[1]}\Gamma_{ri}^{[1]}\xi_{1,s}JH(0) + \eta JG(\mathbf{x}_2-\mathbf{x}_1)(\xi_{2,i}-\xi_{1,i}),\\
\dot{\xi}_{l,i} &= JF(\mathbf{x}_l)\xi_{l,i} - \epsilon\sum_{s=2}^{N}\sum_{r=2}^{N}\Gamma_{rs}^{[l]}\gamma_r^{[l]}\Gamma_{ri}^{[l]}\xi_{l,s}JH(0) + \eta[JG(\mathbf{x}_{l-1}-\mathbf{x}_l)(\xi_{l-1,i}-\xi_{l,i})\\
&\quad + JG(\mathbf{x}_{l+1}-\mathbf{x}_l)(\xi_{l+1,i}-\xi_{l,i})], \quad l=2,3,\ldots,M_1,\\
\dot{\xi}_{M_1+1,i} &= JF(\mathbf{x}_{M_1+1})\xi_{M_1+1,i} - \epsilon\bar{\gamma}_i^{[M_1+1]}JH(0)\xi_{M_1+1,i}\\
&\quad + \eta[JG(\mathbf{x}_{M_1}-\mathbf{x}_{M_1+1})(\xi_{M_1,i}-\xi_{M_1+1,i})\\
&\quad + JG(\mathbf{x}_{M_1+2}-\mathbf{x}_{M_1+1})(\xi_{M_1+2,i}-\xi_{M_1+1,i})],\\
\dot{\xi}_{k,i} &= JF(\mathbf{x}_k)\xi_{k,i} - \epsilon\sum_{s=2}^{N}\sum_{r=2}^{N}\Gamma_{rs}^{[k]}\gamma_r^{[k]}\Gamma_{ri}^{[k]}\xi_{k,s}JH(0) + \eta[JG(\mathbf{x}_{k-1}-\mathbf{x}_k)(\xi_{k-1,i}-\xi_{k,i})\\
&\quad + JG(\mathbf{x}_{k+1}-\mathbf{x}_k)(\xi_{k+1,i}-\xi_{k,i})], \quad k=M_1+2,M_1+3,\ldots,M_1+M_2\\
\text{and}\quad \dot{\xi}_{M_1+M_2+1,i} &= JF(\mathbf{x}_{M_1+M_2+1})\xi_{M_1+M_2+1,i}\\
&\quad - \epsilon\sum_{s=2}^{N}\sum_{r=2}^{N}\Gamma_{rs}^{[M_1+M_2+1]}\gamma_r^{[M_1+M_2+1]}\Gamma_{ri}^{[M_1+M_2+1]}\xi_{M_1+M_2+1,s}JH(0)\\
&\quad + \eta\, JG(\mathbf{x}_{M_1+M_2}-\mathbf{x}_{M_1+M_2+1})(\xi_{M_1+M_2,i}-\xi_{M_1+M_2+1,i}),
\end{aligned}\right\} \tag{3.7}$$

where $i=2,3,\ldots,N$. While $i=1$ yields the linearized equation as

$$\left.\begin{aligned}
&\dot{\xi}_{1,1} = JF(\mathbf{x}_1)\xi_{1,1} + \eta JG(\mathbf{x}_2-\mathbf{x}_1)(\xi_{2,1}-\xi_{1,1}),\\
&\dot{\xi}_{l,1} = JF(\mathbf{x}_l)\xi_{l,1} + \eta[JG(\mathbf{x}_{l-1}-\mathbf{x}_l)(\xi_{l-1,1}-\xi_{l,1}) + JG(\mathbf{x}_{l+1}-\mathbf{x}_l)(\xi_{l+1,1}-\xi_{l,1})],\\
&\quad l=2,3,\ldots,M_1+M_2\\
\text{and}\quad &\dot{\xi}_{M_1+M_2+1,1} = JF(\mathbf{x}_{M_1+M_2+1})\xi_{M_1+M_2+1,1} + \eta\, JG(\mathbf{x}_{M_1+M_2}-\mathbf{x}_{M_1+M_2+1})\\
&\qquad\qquad \times(\xi_{M_1+M_2,1}-\xi_{M_1+M_2+1,1}).
\end{aligned}\right\} \tag{3.8}$$

Clearly, it is the linearized equation of equation (3.2), so it evolves parallel to the synchronization manifold.

If all the time-static Laplacian matrices commute with the time-average Laplacian matrix $\bar{\mathscr{L}}^{[M_1+1]}$, then they can be simultaneously diagonalized by a common basis of orthogonal

eigenvectors. Therefore, we can assume $V^{[k]} = \bar{V}^{[M_1+1]}$ for all k. In turn $\Gamma^{[k]}$ becomes $\mathbb{I}_N$, then we can derive the variational equation for transverse stability of the synchronization manifold as

$$\left.\begin{aligned}
\dot{\xi}_{1,i} &= JF(\mathbf{x}_1)\xi_{1,i} - \epsilon\gamma_i^{[1]}\xi_{1,i}JH(0) + \eta JG(\mathbf{x}_2 - \mathbf{x}_1)(\xi_{2,i} - \xi_{1,i}),\\
\dot{\xi}_{l,i} &= JF(\mathbf{x}_l)\xi_{l,i} - \epsilon\gamma_i^{[l]}\xi_{l,i}JH(0) + \eta[JG(\mathbf{x}_{l-1} - \mathbf{x}_l)(\xi_{l-1,i} - \xi_{l,i})\\
&\quad + JG(\mathbf{x}_{l+1} - \mathbf{x}_l)(\xi_{l+1,i} - \xi_{l,i})],\\
&\quad l = 2, 3, \ldots, M_1,\\
\dot{\xi}_{M_1+1,i} &= JF(\mathbf{x}_{M_1+1})\xi_{M_1+1,i} - \epsilon\bar{\gamma}_i^{[M_1+1]}JH(0)\xi_{M_1+1,i}\\
&\quad + \eta[JG(\mathbf{x}_{M_1} - \mathbf{x}_{M_1+1})(\xi_{M_1,i} - \xi_{M_1+1,i})\\
&\quad + JG(\mathbf{x}_{M_1+2} - \mathbf{x}_{M_1+1})(\xi_{M_1+2,i} - \xi_{M_1+1,i})],\\
\dot{\xi}_{k,i} &= JF(\mathbf{x}_k)\xi_{k,i} - \epsilon\gamma_i^{[k]}\xi_{k,i}JH(0) + \eta[JG(\mathbf{x}_{k-1} - \mathbf{x}_k)(\xi_{k-1,i} - \xi_{k,i})\\
&\quad + JG(\mathbf{x}_{k+1} - \mathbf{x}_k)(\xi_{k+1,i} - \xi_{k,i})], \quad k = M_1 + 2, M_1 + 3, \ldots, M_1 + M_2\\
\text{and}\quad \dot{\xi}_{M_1+M_2+1,i} &= JF(\mathbf{x}_{M_1+M_2+1})\xi_{M_1+M_2+1,i} - \epsilon\gamma_i^{[M_1+M_2+1]}\xi_{M_1+M_2+1,i}JH(0)\\
&\quad + \eta JG(\mathbf{x}_{M_1+M_2} - \mathbf{x}_{M_1+M_2+1})(\xi_{M_1+M_2,i} - \xi_{M_1+M_2+1,i}),
\end{aligned}\right\} \tag{3.9}$$

where $i = 2, 3, \ldots, N$ corresponds to all the transverse directions. Therefore, if the time-static Laplacian matrices are commute with the time-average Laplacian matrix $\bar{\mathscr{L}}^{[M_1+1]}$, then the coupled $(M_1 + M_2 + 1)(N - 1)d$ dimensional transverse error dynamics turns out to be a d-dimensional $(M_1 + M_2 + 1)(N - 1)$ uncoupled error dynamics.

By calculating the Lyapunov exponent, we can measure the exponential expansion or contraction of the above linearized equation transverse to the intralayer synchronization manifold. To determine the stability of the intralayer synchronization state, we need to calculate the maximum transverse Lyapunov exponent Λ (say) which plays a key role. If Λ greater than or equal to zero, the intralayer synchronization state is turnout to be locally unstable. The negative value of Λ indicates the local stability of the intralayer synchronization state. By adjusting the tuning parameters, we trace-out the intralayer synchronization region where the value of Λ is negative.

4. Numerical results

Now, our main emphasis is to verify the above analytical findings by considering two-, three-, four- and five-layers multiplex networks. We systematically study three different types of cases based on the numbers and position of static layers: (i) $M_1 = 1$ and $M_2 = 0$, two-layered multiplex network with one layer time varying and other static layer, (ii) $M_1 = M_2$, i.e. the middle layer is time varying, the upper and lower layers are time invariant (iii) $M_1 \neq M_2 \neq 0$, i.e. the number of time-static layers with respect to the time-varying layer are not symmetric. The intralayer synchronization error E for the l-layer multiplex network is defined as

$$E = \frac{1}{M_1 + M_2 + 1}\sum_{l=1}^{M_1+M_2+1} E_l, \quad \text{where } E_l = \lim_{T\to\infty}\frac{1}{T}\int_0^T \sum_{j=2}^{N}\frac{\|\mathbf{x}_{l,j}(t) - \mathbf{x}_{l,1}(t)\|}{N-1}\,\mathrm{d}t$$

is the synchronization error in each layer and $\|\cdot\|$ denotes the Euclidean norm. Each layer of the dynamical multiplex network possesses an Erdös-Rényi (ER) random network with $N = 200$ nodes in each layer. The local dynamics of each node is associated with paradigmatic chaotic Lorenz oscillator with the evolution equation $F(\mathbf{x}) = [\sigma(y - x), x(\rho - z) - y, xy - \beta z]^{tr}$. Here, tr stands for the transpose of the vector. The system parameter values, $\sigma = 10$, $\rho = 28$ and $\beta = 8/3$ are fixed and described a chaotic regime. The random network probabilities of the static and time-varying layers are chosen as p_1 and p_2, respectively. We integrate the ordinary differential equations by using the fourth-order Runge–Kutta method with the integration time step $\mathrm{d}t = 0.01$.

For our entire numerical simulations, the time interval is taken over 3×10^5 units after an initial transient of 2×10^5 units. The fixed initial conditions are chosen from the phase space volume of the Lorenz system. To draw the following parameter regions, we have taken 10 network realizations at each point.

(a) Two-layers multiplex network ($M_1 = 1, M_2 = 0$)

We start our investigation by considering two-layered multiplex networks. For layer-1, we consider the interlayer coupling as a temporal random network with probability p_1, and for layer-2, we again consider a random network, but static with probability p_2. Then the time-average Laplacian matrix $\mathscr{L}^{(1)}$ becomes $\bar{\mathscr{L}}^{(1)}_{ij} = -p_1$ for $i \neq j$ and $(N-1)p_1$ for $i = j$. It is easy to check that $\bar{\mathscr{L}}^{(1)}$ is a symmetric circulant matrix. So its N eigenvalues are $\sum_{m=1}^{N} \bar{\mathscr{L}}^{(1)}_{1m} \omega_j^{m-1}$ for $0 \leq j \leq N-1$, where $\omega_j = \exp((2\pi j\sqrt{-1})/N)$, which yields N eigenvalues as $Np - p\sum_{m=0}^{N-1} \omega_j^m$. Therefore, the different eigenvalues of $\bar{\mathscr{L}}^{(1)}$ are 0 and Np.

The intralayer synchronization transition scenarios of equation (2.1) are shown in figure 2. Figure 2*a* depicts the temporal evolution of the two-layers multiplex network for the intralayer coupling strength $\epsilon = 3.0$, interlayer coupling strength $\eta = 0.6$, rewiring probability $p_r = 0.001$ and random network probabilities $p_{1,2} = 0.05$. From this figure, we observe that after a few transient periods, all the oscillators in each layer separately converge to the intralayer synchronization solutions, which is consistent only with the complete synchronization of each layer. The green and blue curves in figure 2*a* are the complete synchronous solutions in each layer. The synchronization error for the complete intralayer synchrony of the two-layers multiplex network is plotted in figure 2*b* for the fixed rewiring probability $p_r = 0.001$. The solid (dashed) curves represent the variation of the intralayer synchrony error E_1 (E_2) for time-varying layer and static layer, respectively. The blue curves in figure 2*b* are plotted when both layers are uncoupled, i.e. for $\eta = 0.0$. In the absence of the interlayer interaction, the critical synchrony threshold for two identical layers occurs at different values of ϵ, for the time-varying layer, $\epsilon \simeq 3.0$, and the static layer, $\epsilon \simeq 5.0$. So, the time-varying character (in layer-1) enhances the complete synchrony threshold compared to the static layer and hence two layers synchronize for two different values of ϵ. For the presence of the interlayer connections, two coupled layers synchronize and desynchronize simultaneously. The red and green curves in figure 2*b* represent intralayer synchrony of two individual layers for lower and sufficient higher interlayer coupling values at $\eta = 0.001$ and $\eta = 5.0$. For a very low value of $\eta = 0.001$, both layers synchronize simultaneously at $\epsilon \simeq 5.0$. But for sufficient larger values $\eta = 5.0$, both layers synchronize at lower values of the $\epsilon \simeq 2.2$ as both errors $E_{1,2}$ become zero simultaneously at this ϵ critical value. Although in the multiplex network one layer is time varying yet two layers synchronize simultaneously when they are coupled. 'So, it is concluded that the combined effect of time-varying features in one layer and the presence of interlayer links between the layers lead to the simultaneous appearance of synchronization states as well as an induced enhancement of intralayer synchrony'.

In order to reveal the combined effect of the rewiring probability p_r and the intralayer coupling strength ϵ on the transition of the intralayer synchrony, we have drawn a phase diagram in the (ϵ, p_r) plane in figure 2*c* for a fixed $\eta = 5.0$. The colour bar denotes the variation of the intralayer synchronization error E. Here, larger values of the rewiring probability p_r gradually decrease the critical synchrony threshold ϵ. This means when two layers are almost static, then higher intralayer coupling values are needed for reaching intralayer synchrony, but when the intralayer links of one layer is rewired sufficiently fast (that is higher p_r values), then the critical threshold of ϵ is enhanced for both time-varying and static layers. Similarly, in figure 2*d*, the simultaneous influence of intralayer and interlayer coupling strengths is presented in the (ϵ, η) parameter space for the fixed rewiring probability $p_r = 0.001$. When two layers are uncoupled, i.e. $\eta = 0.0$, then intralayer synchronization occurs after $\epsilon = 5.0$. But when we couple two layers and gradually increase the value of η, then the critical values of ϵ for synchrony are smoothly decreasing. From this picture, one can conclude that the interlayer interaction strength and the temporal features

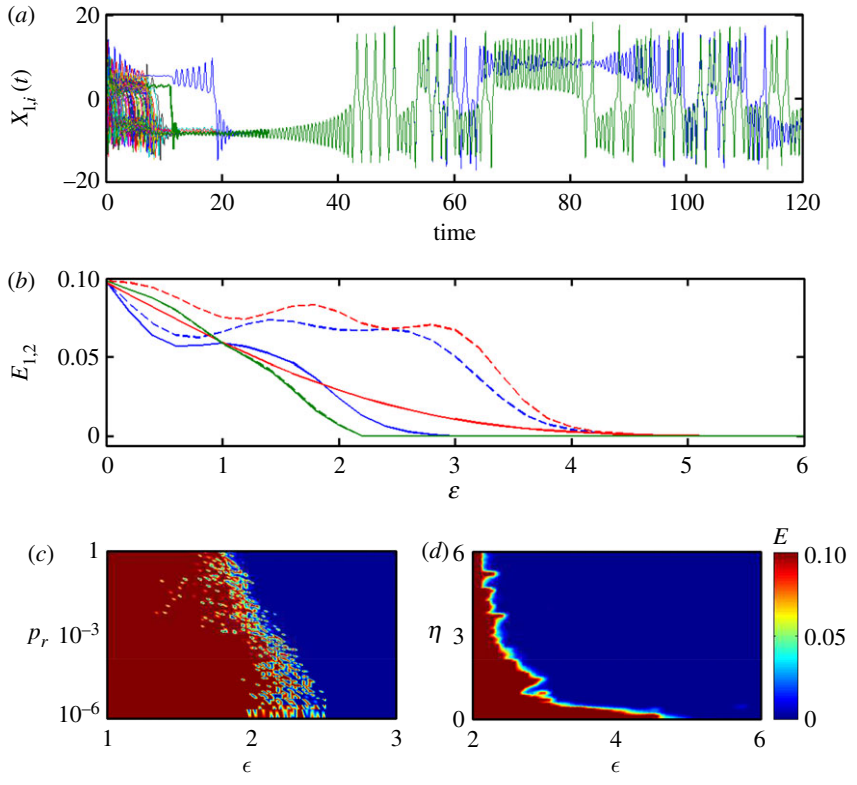

Figure 2. Two-layers multiplex network: (*a*) time evolution of the intralayer synchronization states for $\epsilon = 3.0$, $\eta = 0.6$ and $p_r = 0.001$. (*b*) Complete synchronization errors E_1 (solid curves) and E_2 (dashed curves) of the time-varying and static layers with respect to ϵ for $\eta = 0.0$ (blue curves), $\eta = 0.001$ (red curves) and $\eta = 5.0$ (green curves). Rewiring probability is fixed at $p_r = 0.001$. Variation of E in the parameter space of (*c*) (ϵ, p_r) for $\eta = 5.0$, and (*d*) (ϵ, η) for $p_r = 0.001$. The ER probability for the two layers are fixed at $p_{1,2} = 0.05$. (Online version in colour.)

in one layer play a key role in the emergence and enhancement of intralayer synchrony in the multiplex network.

For this time-varying two-layers network, we can write the equation of motion of the intralayer synchronization solution as: (Layer-1) $\dot{x}_1 = \sigma(y_1 - x_1)$, $\dot{y}_1 = x_1(\rho - z_1) - y_1 + \eta(y_2 - y_1)$, $\dot{z}_1 = x_1 y_1 - \beta z_1$, and (Layer-2) $\dot{x}_2 = \sigma(y_2 - x_2)$, $\dot{y}_2 = x_2(\rho - z_2) - y_2 + \eta(y_1 - y_2)$, $\dot{z}_2 = x_2 y_2 - \beta z_2$. For sufficient fast switching, the transverse error dynamics of the intralayer synchronization manifold becomes

$$\left.\begin{aligned}
\dot{\xi}^{(x)}_{1,i} &= \sigma(\xi^{(y)}_{1,i} - \xi^{(x)}_{1,i}) - \epsilon N p \xi^{(x)}_{1,i},\\
\dot{\xi}^{(y)}_{1,i} &= \xi^{(x)}_{1,i}(\rho - z_1) - x_1 \xi^{(z)}_{1,i} - \xi^{(y)}_{1,i} + \eta(\xi^{(y)}_{2,i} - \xi^{(y)}_{1,i}),\\
\dot{\xi}^{(z)}_{1,i} &= \xi^{(x)}_{1,i} y_1 + x_1 \xi^{(y)}_{1,i} - \beta \xi^{(z)}_{1,i},\\
\dot{\xi}^{(x)}_{2,i} &= \sigma(\xi^{(y)}_{2,i} - \xi^{(x)}_{2,i}) - \epsilon \gamma^{(2)}_i \xi^{(x)}_{2,i},\\
\dot{\xi}^{(y)}_{2,i} &= \xi^{(x)}_{2,i}(\rho - z_2) - x_2 \xi^{(z)}_{2,i} - \xi^{(y)}_{2,i} + \eta(\xi^{(y)}_{1,i} - \xi^{(y)}_{2,i})\\
\text{and}\quad \dot{\xi}^{(z)}_{2,i} &= \xi^{(x)}_{2,i} y_{2,i} + x_2 \xi^{(y)}_{2,i} - \beta \xi^{(z)}_{2,i},
\end{aligned}\right\} \tag{4.1}$$

where $i = 2, 3, \ldots, N$; $(\xi^{(x)}_{1,i}, \xi^{(y)}_{1,i}, \xi^{(z)}_{1,i}, \xi^{(x)}_{2,i}, \xi^{(y)}_{2,i}, \xi^{(z)}_{2,i})$ is the projected error component.

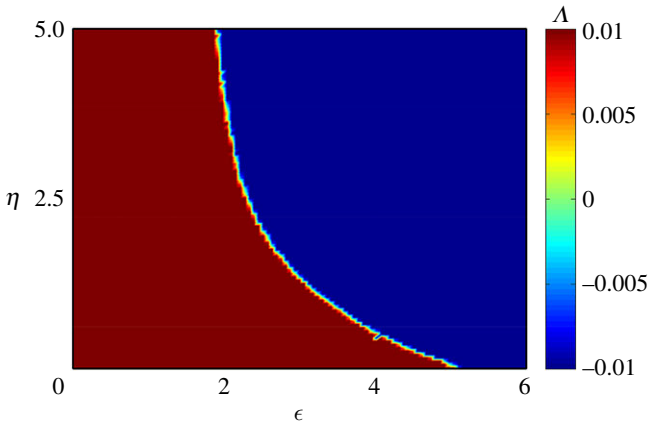

Figure 3. Two-layers multiplex network: variation of maximum transverse Lyapunov exponent Λ in the (ϵ, η) parameter plane for sufficient fast switching. The ER random probabilities for two layers are fixed at $p_1 = p_2 = 0.05$. (Online version in colour.)

Now, we investigate the stability of intralayer synchronization states of the multiplex network using the maximum transverse Lyapunov exponent. The existence criterion for the intralayer synchronization manifold is analytically derived by a linear stability analysis in terms of the MSF approach. In figure 3, the transition from desynchrony to synchrony is characterized by the maximum transverse Lyapunov exponent Λ in the (ϵ, η) parameter space. The colour bar denotes the variation of Λ. The stability of the intralayer synchrony is characterized by $\Lambda < 0$. Here, a monotonic enhancement with respect to both varying parameters is observed. For $\eta = 0$, that is, when both layers are uncoupled, the intralayer synchronization achieves at $\epsilon \simeq 5.0$. Due to the interaction between both layers, the complete synchronization in each layer appears together and is enhanced monotonically. Finally, for $\eta = 5.0$, intralayer synchronization achieves at $\epsilon = 1.92$. So our fast switching stability analysis quite well agrees with the (ϵ, η) parameter space of the synchronization error of figure 2*d*.

Next, the combined effect of the ER random probabilities p_1 and p_2 for time-varying and static layers is studied for the transition scenarios of the intralayer synchrony. By considering the various illustrated values of the intralayer and interlayer couplings, the synchrony and desynchrony regions are drawn in the (p_1, p_2) parameter space in figure 4. The upper panel (figure 4*a*,*b*) is drawn for the fixed intralayer coupling strength $\epsilon = 3$ and two different interlayer coupling values as $\eta = 1.5$ and $\eta = 3.5$, respectively. Similarly, for the fixed interlayer interaction strength $\eta = 2.5$, the synchrony and desynchrony regions are plotted in figure 4*c*,*d* for respective values of $\epsilon = 3.0$ and $\epsilon = 6.0$. The blue region corresponds to the intralayer synchronization region. Here, we observe a significant variation of the synchronization region against the tuning parameters ϵ and η. Interestingly, note that the upper threshold of these two $p_{1,2}$ values are not much changed with the different set of intralayer and interlayer coupling values, while the lower values of p_1 and p_2 have a mutual effect on the synchronization transition.

(b) Three-layers multiplex network ($M_1 = 1, M_2 = 1$)

Now, we investigate the effect of one time-varying layer in a three-layers multiplex network. In this multiplex architecture, we keep only the middle layer as the time-varying layer, while the upper and lower layers are time invariant. The network topologies of all the layers are ER random networks. Here, the p_1 and p_2 represents the ER probability for static and temporal layers respectively. Using temporal evaluation and different characterizations as synchrony error and Lyapunov spectrum, we uncovered the synchronization transition scenarios in figures 5–7.

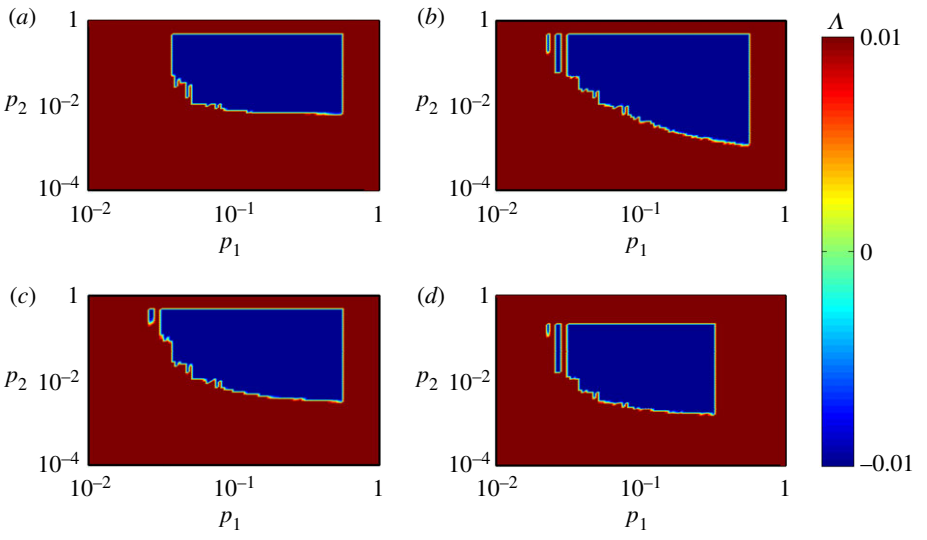

Figure 4. Two-layers multiplex network: variation of Λ in the (p_1, p_2) parameter space where the intra- and interlayer interaction strengths are (*a*) $\epsilon = 3.0$, $\eta = 1.5$, (*b*) $\epsilon = 3.0$, $\eta = 3.5$, (*c*) $\epsilon = 3.0$, $\eta = 2.5$ and (*d*) $\epsilon = 6.0$, $\eta = 2.5$. (Online version in colour.)

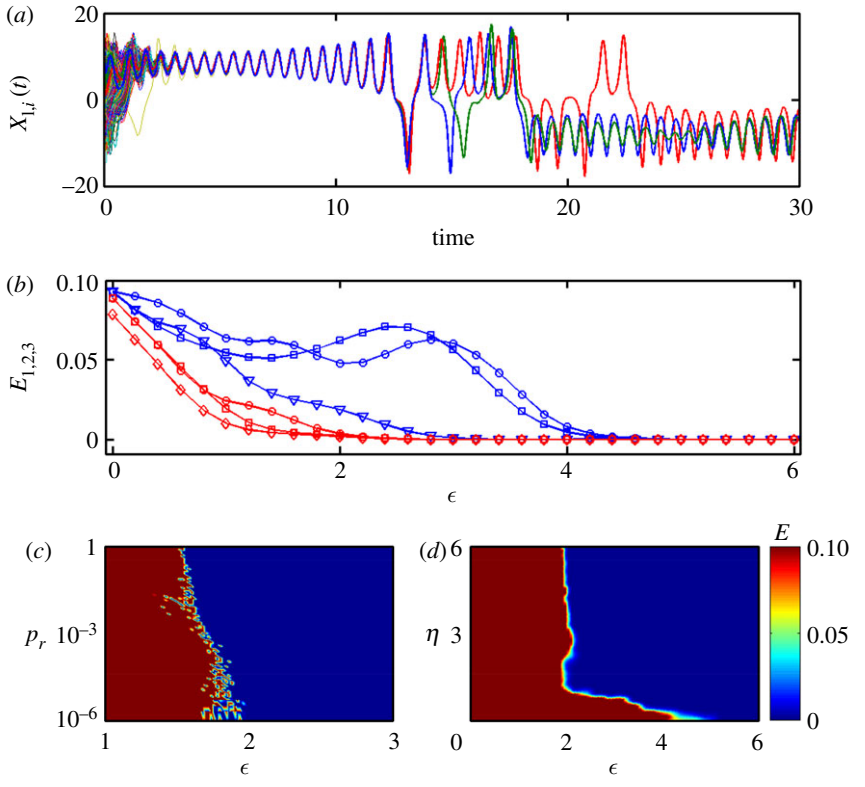

Figure 5. Three-layers multiplex network: (*a*) time series of the two synchronized layer for $\epsilon = 3.0$, $\eta = 0.6$ and $p_r = 0.001$. (*b*) Complete synchronization errors E_1 (line with circles), E_2 (line with triangles), E_3 (line with squares) of the three-layers with respect to ϵ for $\eta = 0$ (blue curves) and $\eta = 0.7$ (red curves). Variation of the intralayer synchronization error E in the parameter space of (*c*) (ϵ, p_r) for $\eta = 5.0$, and (*d*) (ϵ, η) for $p_r = 0.001$. Other parameters: $p_{1,2} = 0.05$. (Online version in colour.)

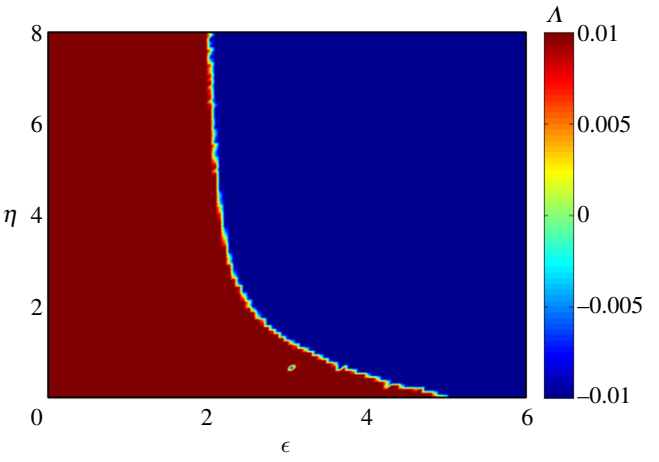

Figure 6. Three-layers multiplex network: variation of Λ in the (ϵ, η) parameter space for three-layers multiplex network. Here, $p_1 = p_2 = 0.05$. (Online version in colour.)

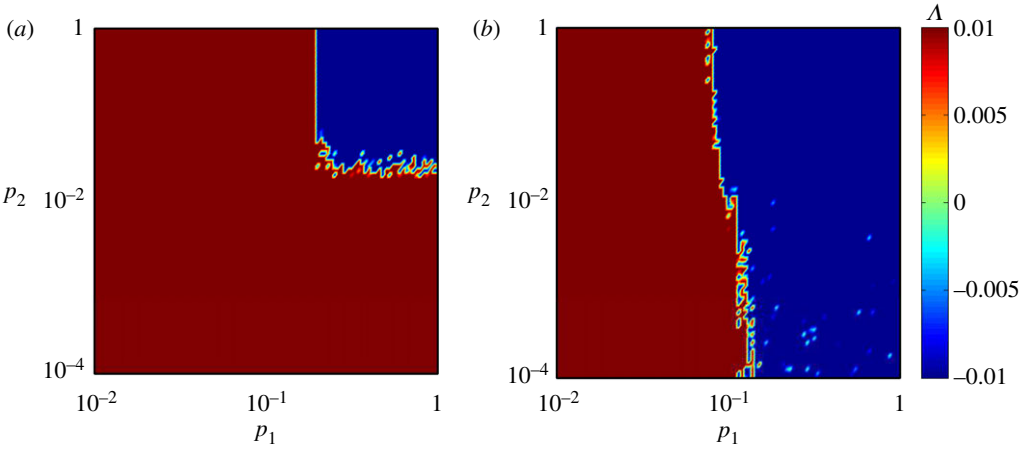

Figure 7. Three-layers multiplex network: maximum transverse Lyapunov exponent Λ of the intralayer synchronization state in (p_1, p_2) parameter space for (*a*) $\epsilon = 0.3$, $\eta = 0.3$ and (*b*) $\epsilon = 0.6$, $\eta = 0.6$. The blue and red colours correspond to the synchrony and desynchrony regions, respectively. (Online version in colour.)

Figure 5*a* shows the temporal evolution of the intralayer synchronization states for the three different layers with fixed $\epsilon = 3.0$ and $\eta = 0.6$ and rewiring probability $p_r = 0.001$. After a finite transient time, all the nodes in the respective layer converge to the synchronization solutions. Here, the red curve represents the complete intralayer synchronization solutions of the time-varying layers, while the blue and green ones correspond to the time-invariant layers. The complete intralayer synchronization errors E_1 (line with circles), E_2 (line with triangles) and E_3 (line with squares) of the three layers are drawn against ϵ in figure 5*b*. The solid triangle curve denotes the intralayer synchrony error for the time-varying layer, while the other two curves represent the intralayer synchrony errors for the static layers. Similar to the two-layer case, here also the time-varying layer is synchronized at lower values of $\epsilon \simeq 3.0$ compared to the synchrony threshold ($\epsilon \simeq 5.0$) of the static layer in the absence of the interlayer interaction ($\eta = 0.0$). The results are presented by the blue colour synchronization error in figure 5*b*. But when the interlayer coupling strength $\eta \neq 0$ among the three layers, the intralayer synchrony appears simultaneously and for sufficient large values of η, an enhancement of the intralayer synchrony is observed. In

the presence of interlayer links, the intralayer synchrony errors were plotted (red colour line) in figure 5*b*. At $\eta \simeq 0.7$, complete synchronization of the three layers occurs at $\epsilon \simeq 2.8$ which is much lower compared to any uncoupled intralayer synchrony threshold. So depending on the interlayer coupling strength, the time-varying features in one layer compelled to the other two layers for achieving intralayer synchrony and also the temporal behaviour plays an important role for the enhancement of their synchrony bound. Next, we draw the intralayer synchronization and desynchronization regions in figure 5*c* in the (ϵ, p_r) parameter plane for fixed $\eta = 5.0$ and random probabilities $p_{1,2} = 0.05$. Here, the intralayer synchronization monotonically enhances the intralayer coupling values by increasing the rewiring probability of the time-varying layer. To investigate the effect of the interlayer coupling strength η on the transition of the intralayer synchronization state, we plot E in the (ϵ, η) parameter space in figure 5*d* for fixed $p_r = 0.001$. First, by gradually increasing η, the critical synchrony threshold of ϵ is monotonically decreasing and this enhancement occurs up to a certain value of ϵ. After that, there is not much effect of the interlayer couplings on the enhancement of the intralayer synchrony threshold.

By using the fast switching criterion, we analyse the stability of the intralayer synchrony analytically. Numerically, we plot the maximum Lyapunov exponent Λ of the transverse error systems in figure 6 by simultaneously varying ϵ and η for the sufficient fast switching case. Here, we keep the random probabilities for time-varying and static layer at $p_{1,2} = 0.05$. The blue colour denotes the synchrony region where $\Lambda < 0$. Here, we observe a monotonic enhancement with respect to both varying parameters up to a certain range of ϵ and η. After particular values of η, no enhancement for ϵ values was observed in figure 6. The intralayer synchrony characterization presented in figure 6 is in agreement with the results of figure 5*d*.

To investigate the effect of the probability on the intralayer synchrony of the static and time-varying random network, we plot Λ in the (p_1, p_2) parameter space in figure 7 with a fixed set of values of the intralayer and interlayer coupling strengths. Figure 7*a*,*b* is drawn for the set of ($\epsilon = 0.3$, $\eta = 0.3$) and ($\epsilon = 0.6$, $\eta = 0.6$), respectively. Interestingly, here it is observed that for the lower set of values of the interaction strength, synchronization can only appear for higher values of both probabilities p_1 and p_2 of the random networks. For slight higher values of ϵ and η in figure 7*b*, we find that synchronization can be achieved by only increasing the probability of the static layers. So, higher values of both interaction strengths lead to the emergence of a larger window of the synchrony region in the (p_1, p_2) parameter space.

(c) Four-layers multiplex network ($M_1 = 1, M_2 = 2$)

In this subsection, we numerically explore intralayer synchrony in a four-layers multiplex network in different parameter spaces. Here, we consider $M_1 = 1$ and $M_2 = 2$, therefore, the second layer is the time-varying layer, and the remaining other layers are static. The intralayer network architectures for all the layers are chosen as ER random network. The random network probabilities of the time-varying and static layers are denoted by p_1 and p_2, respectively.

For the $p_r = 0.001$, the variation of E in the (ϵ, p_r) parameter space is depicted in figure 8*a*. Here, the interlayer coupling strength is fixed at $\eta = 5.0$ and $p_{1,2} = 0.05$. The intralayer synchronization enhances with respect to both varying parameters ϵ and p_r. For a very slow switching network, i.e. $p_r \sim 10^{-6}$, the critical transition from desynchrony to synchrony occurs at $\epsilon \simeq 1.85$. Further increasing the rewiring probability only in the second layer yields an enhancement of the complete synchrony in all other layers. Figure 8*b* represents the intralayer synchrony scenario in terms of the synchronization error E in the parameter space (ϵ, η). The increasing values of the interlayer synchrony up to a certain threshold promotes the enhancement of the intralayer synchrony. Beyond this value of η, no further enhancement of ϵ was observed. That means, after a certain threshold of interlayer coupling strength, it has no effect on the emergence of intralayer synchrony.

Next, for a fast switching intralayer network in the second layer, the stability of the synchronization states are presented in figure 9 in terms of Λ. A monotonic enhancement of the intralayer synchronization is observed in this parameter space. The critical values of intralayer

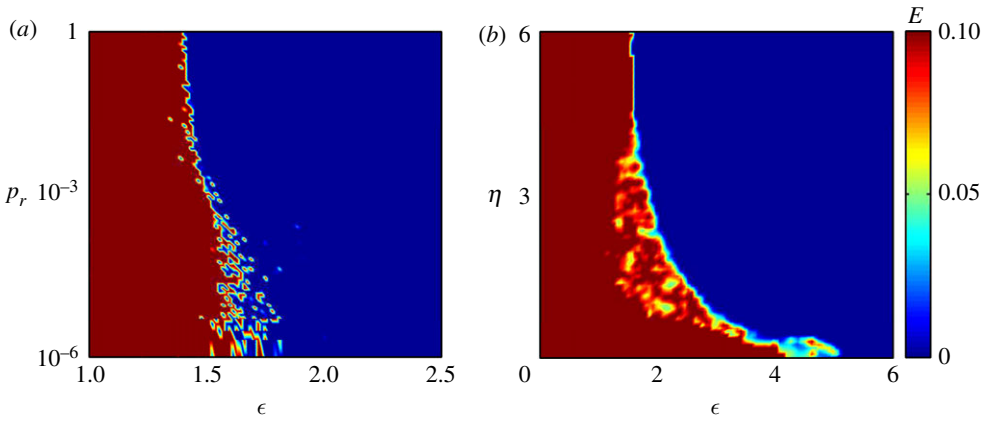

Figure 8. Four-layers multiplex network: variation of intralayer synchronization error in the parameter space of (*a*) (ϵ, p_r) with $\eta = 5.0$ and (*b*) (ϵ, η) for $p_r = 0.001$. Other parameters: $p_{1,2} = 0.05$. (Online version in colour.)

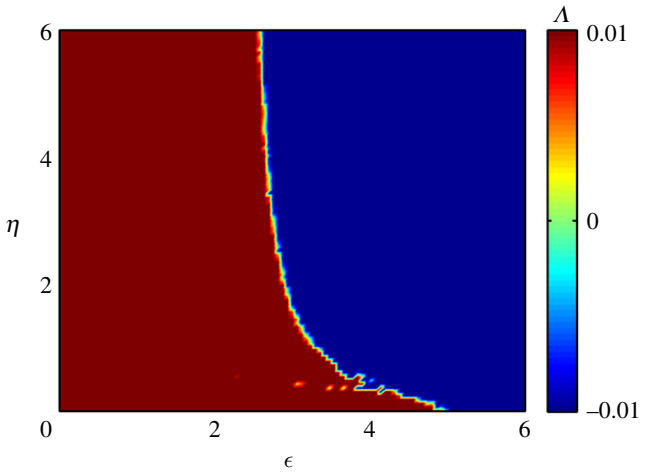

Figure 9. Four-layers multiplex network: variation of Λ for four layered multiplex network in the parameter space of (ϵ, η) for $p_{1,2} = 0.05$. (Online version in colour.)

coupling strength ϵ is monotonically enhanced by gradually increasing the interlayer interaction strength η of the four-layers network.

(d) Five-layers multiplex network ($M_1 = 2, M_2 = 2$)

Finally, we numerically investigate intralayer synchrony phenomena in a five-layers multiplex network to verify the universality of our analytical finding of the generalized multiplex network. In the five-layers multiplex network, we keep only the middle layer as time varying and the remaining two upper and lower layers are static. For the numerical simulation purpose, we chose the intralayer network topologies for all the layers as random networks.

Figure 10*a* depicts the intralayer synchronization error in the (ϵ, η) parameter space for the fixed rewiring probability of the middle layer $p_r = 0.001$. For this moderate switching multiplex network, when all the layers are uncoupled, the intralayer synchronization occurs at $\epsilon = 5.0$. First, gradually increasing η, the critical intralayer coupling strength monotonically decreases, which means an enhancement of ϵ occurs. At $\eta = 1.0$, the intralayer synchronization occurs at

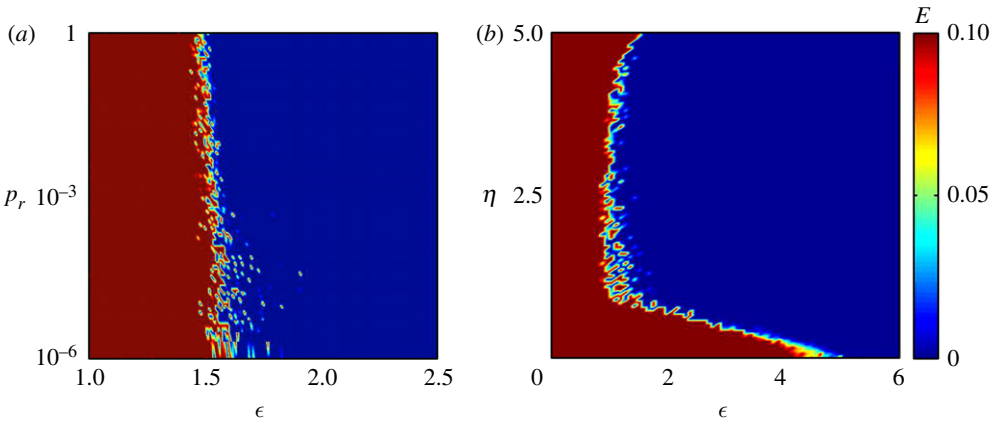

Figure 10. Five-layers multiplex network: intralayer synchronization error in the parameter space of (*a*)(ϵ, p_r) with $\eta = 8.0$ and (*b*) (ϵ, η) with $p_r = 0.001$. Other parameters: $p_{1,2} = 0.05$. (Online version in colour.)

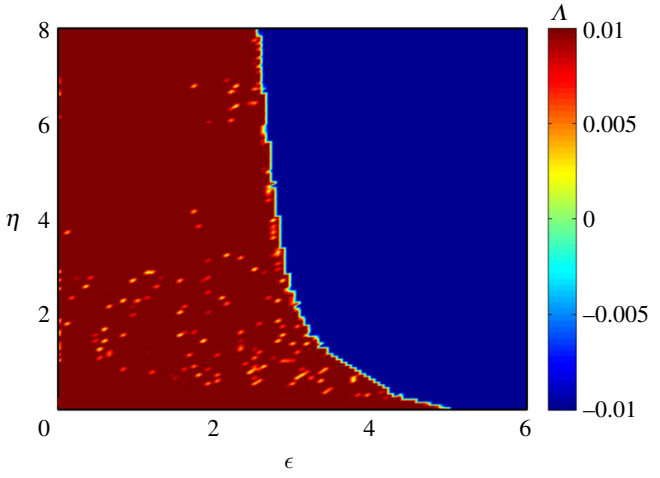

Figure 11. Variation of Λ for five layered multiplex network in the parameter space of (ϵ, η) for $p_{1,2} = 0.05$. (Online version in colour.)

$\epsilon \simeq 1.35$, and a further increasing of the values of η, the critical values of ϵ enhances up to 1.1. Beyond this value of η, no further enhancement of ϵ was observed. That means, after a certain threshold of the interlayer coupling strength, it has no effect on the emergence of intralayer synchrony. Next, we uncover the effect of the rewiring probability in figure 10*b* on the transition of intralayer synchrony. For fixed $p_{1,2} = 0.05$ and $\eta = 8.0$, the synchrony error is calculated in the (ϵ, p_r) parameter plane. By increasing the rewiring probability from 10^{-6} to 10^{0}, the intralayer synchronization enhances with respect to ϵ. For a slow switching network, i.e. $p_r = 10^{-6}$ the critical transition occurs at $\epsilon = 1.65$ and for fast rewiring, i.e. for $p_r = 10^{0}$ it enhances to $\epsilon = 1.5$. Switching the intralayer links in only one layer promotes the entire multiplex network for enhancement of the intralayer synchrony.

Next, for a fast switching network, we analyse the stability of the intralayer synchronization states by our derived fast switching stability criterion. In figure 11, we plot the maximum transverse Lyapunov exponent in the (ϵ, η) parameter space where the colour bar denotes the variation of Λ. In this parameter space, a monotonous enhancement of the intralayer

synchronization is observed. By gradually increasing the interlayer interaction strength η of the five-layers network, the critical values of the intralayer coupling strength ϵ is monotonically enhancing.

5. Conclusion

We have investigated complete intralayer synchrony under the influence of the coexistence of static and time-varying layers in a multiplex formulation. The interlayer links and the intralayer connections of all layers (except the time-varying layer) are time static. In the time-varying layer, the intralayer links are allowed to change stochastically over time with a certain rewiring frequency. We have started our study by considering two-layers multiplex networks where the intralayer link in one layer possesses time-varying features and in the other layer, it is static and the interlayer connection is always time invariant. The temporal feature plays a key role for the enhancement of synchrony in a time-varying dynamical network. But surprisingly, here we have found that the time-varying characteristic induces an enhancement of synchrony depending on the interlayer coupling strength. Here, multiplexing also plays a crucial role in obtaining a critical threshold for the intralayer synchrony in the individual layers. So, it is important to investigate the effect of the number of layers on the synchrony property. To establish our analytical findings, we have extended our study by considering more number of layers in the multiplex networks, namely three, four and five layers. Detailed transition scenarios from desynchrony to synchrony under the effect of rewiring frequency and both coupling values are discussed in a wide range of different parameter spaces.

We have analytically derived necessary and sufficient conditions for the existence of the intralayer synchronization manifold by using the MSF approach for fast switching of the rewiring frequency. For sufficiently fast switching, a time-varying network is approximated by a time-averaged network and also, we have approximated our time-varying multilayer network by a static time-average multilayer network. We have generalized our stability theory to an independent number of layers in the multiplex network. Our numerical results are in excellent agreement with our theoretical findings. For the numerical simulations, each node of the network is modelled by the paradigmatic chaotic Lorenz oscillator and the corresponding Erdős-Rényi random network is considered in each layer.

Data accessibility. The codes to generate figures of this article have been uploaded as part of the electronic supplementary material.

Authors' contributions. All authors equally contributed and gave the final approval for the publication.

Competing interests. We declare we have no competing interests.

Funding. No funding has been received for this article.

References

1. Albert R, Barabási AL. 2002 Statistical mechanics of complex networks. *Rev. Mod. Phys.* **74**, 47–97. (doi:10.1103/RevModPhys.74.47)
2. Kivelä M, Arenas A, Barthelemy M, Gleeson JP, Moreno Y, Porter MA. 2014 Multilayer networks. *J. Complex Netw.* **2**, 203–271. (doi: 10.1093/comnet/cnu016)
3. Bianconi G. 2018 *Multilayer networks: structure and function*. Oxford, UK: Oxford University Press.
4. Gao J, Li D, Havlin S. 2014 From a single network to a network of networks. *Natl Sci. Rev.* **1**, 346–356. (doi:10.1093/nsr/nwu020)
5. Kao TC, Porter MA. 2018 Layer communities in multiplex networks. *J. Stat. Phys.* **173**, 1286–1302. (doi:10.1007/s10955-017-1858-z)
6. Barrat A, Barthelemy M, Vespignani A. 2008 *Dynamical processes on complex networks*. Cambridge, UK: Cambridge University Press.
7. Majhi S, Ghosh D. 2017 Amplitude death and resurgence of oscillation in network of mobile oscillators. *Europhys. Lett.* **118**, 40002. (doi:10.1209/0295-5075/118/40002)

8. Pikovsky A, Kurths J, Rosenblum M. 2013 *Synchronization: a universal concept in nonlinear sciences*. Cambridge, UK: Cambridge University Press.
9. Majhi S, Ghosh D. 2017 Synchronization of moving oscillators in three dimensional space. *Chaos* **27**, 053115. (doi:10.1063/1.4984026)
10. Sun J, Bollt EM, Porter MA, Dawkins MS. 2011 A mathematical model for the dynamics and synchronization of cows. *Physica D* **240**, 1497–1509. (doi:10.1016/j.physd.2011.06.009)
11. Kramer S, Bollt EM. 2013 Spatially dependent parameter estimation and nonlinear data assimilation by autosynchronization of a system of partial differential equations. *Chaos* **23**, 033101. (doi:10.1063/1.4812722)
12. Jalan S, Singh A. 2016 Cluster synchronization in multiplex networks. *Europhys. Lett.* **113**, 30002. (doi:10.1209/0295-5075/113/30002)
13. Sevilla-Escoboza R, Sendiña-Nadal I, Leyva I, Gutiérrez R, Buldú JM, Boccaletti S. 2016 Inter-layer synchronization in multiplex networks of identical layers. *Chaos* **26**, 065304. (doi:10.1063/1.4952967)
14. Majhi S, Ghosh D, Kurths J. 2019 Emergence of synchronization in multiplex networks of mobile Rössler oscillators. *Phys. Rev. E* **99**, 012308. (doi:10.1103/PhysRevE.99.012308)
15. Gambuzza LV, Frasca M, Gómez-Gardeñes J. 2015 Intra-layer synchronization in multiplex networks. *Europhys. Lett.* **110**, 20010. (doi:10.1209/0295-5075/110/20010)
16. Rakshit S, Majhi S, Bera BK, Sinha S, Ghosh D. 2017 Time-varying multiplex network: intralayer and interlayer synchronization. *Phys. Rev. E* **96**, 062308. (doi:10.1103/PhysRevE.96.062308)
17. Rakshit S, Bera BK, Ghosh D. 2018 Synchronization in a temporal multiplex neuronal hypernetwork. *Phys. Rev. E* **98**, 032305. (doi:10.1103/PhysRevE.98.032305)
18. Maksimenko VA, Makarov VV, Bera BK, Ghosh D, Dana SK, Goremyko MV, Frolov NS, Koronovskii AA, Hramov AE. 2016 Excitation and suppression of chimera states by multiplexing. *Phys. Rev. E* **94**, 052205. (doi:10.1103/PhysRevE.94.052205)
19. Majhi S, Perc M, Ghosh D. 2016 Chimera states in uncoupled neurons induced by a multilayer structure. *Sci. Rep.* **6**, 39033. (doi:10.1038/srep39033)
20. Majhi S, Perc M, Ghosh D. 2017 Chimera states in a multilayer network of coupled and uncoupled neurons. *Chaos* **27**, 073109. (doi:10.1063/1.4993836)
21. Zhang X, Boccaletti S, Guan S, Liu Z. 2015 Explosive synchronization in adaptive and multilayer networks. *Phys. Rev. Lett.* **114**, 038701. (doi:10.1103/PhysRevLett.114.038701)
22. Holme P, Saramäki J. 2012 Temporal networks. *Phys. Rep.* **519**, 97–125. (doi:10.1016/j.physrep.2012.03.001)
23. Stilwell DJ, Bollt EM, Roberson DG. 2006 Sufficient conditions for fast switching synchronization in time-varying network topologies. *SIAM J. Appl. Dyn. Syst.* **5**, 140–156. (doi:10.1137/050625229)
24. Rakshit S, Bera BK, Ghosh D, Sinha S. 2018 Emergence of synchronization and regularity in firing patterns in time-varying neural hypernetworks. *Phys. Rev. E* **97**, 052304. (doi:10.1103/PhysRevE.97.052304)
25. Nag Chowdhury S, Ghosh D. 2019 Synchronization in dynamic network using threshold control approach. *Europhys. Lett.* **125**, 10011. (doi:10.1209/0295-5075/125/10011)
26. Nag Chowdhury S, Majhi S, Ozer M, Ghosh D, Perc M. 2019 Synchronization to extreme events in moving agents. *New J. Phys.* **21**, 073048. (doi:10.1088/1367-2630/ab2a1f)
27. Banerjee R, Ghosh D, Padmanaban E, Ramaswamy R, Pecora LM, Dana SK. 2012 Enhancing synchrony in chaotic oscillators by dynamic relaying. *Phys. Rev. E* **85**, 027201. (doi:10.1103/PhysRevE.85.027201)
28. Banerjee R, Bera BK, Ghosh D, Dana SK. 2017 Enhancing synchronization in chaotic oscillators by induced heterogeneity. *Eur. Phys. J. Spec. Top.* **226**, 1893–1902. (doi:10.1140/epjst/e2017-70027-9)
29. Dhamala M, Jirsa VK, Ding M. 2004 Enhancement of neural synchrony by time delay. *Phys. Rev. Lett.* **92**, 074104. (doi:10.1103/PhysRevLett.92.074104)
30. Pecora LM, Carroll TL. 1998 Master stability functions for synchronized coupled systems. *Phys. Rev. Lett.* **80**, 2109–2112. (doi:10.1103/PhysRevLett.80.2109)

Supplementary Materials

Enhancing synchrony in multiplex network due to rewiring frequency

Sarbendu Rakshit[1], Bidesh K. Bera[2], Jürgen Kurths[3] and Dibakar Ghosh[1]

[1]Physics and Applied Mathematics Unit, Indian Statistical Institute, 203 B. T. Road, Kolkata-700108, India
[2]Department of Mathematics, Indian Institute of Technology Ropar, Punjab-140001, India
[3]Potsdam Institute for Climate Impact Research, Potsdam 14473, Germany

The following code for the synchronization error with two layer multiplex network.

```
#include <stdio.h>
#include <stdlib.h>
#include <math.h>
main()
{
srand(time(NULL));
int A1[201][201],A2[201][201],IRAND,i4,TT,i,j,j1,ii,n,m,mm,j2,j3,i1,k1,p,i2,i3,tn;
float x20[201],x2[201],y20[201],y2[201],z20[201],z2[201],x10[201],x1[201],y10[201],y1[201],z10[201],z1[201],
k[4][1201],sum2, RAND,sum3,prand,avger,sum1,w0,h,l,w,sigma,beta,rho,eps,eta,error,rf,rp,np,er1,er2;

FILE *fopen(),*fp1,*fp2;
fp1=fopen("L_M_ts.out","w");
fp2=fopen("L_M_2l_eps_eta_E_1.out","w");
n=200; //Number of nodes in each layer
mm=500000;// Time Iteration
tn=200000;// Transient
TT=50; // Network Realization
sigma=10.0; beta=8.0/3.0; rho=28.0;
prand=0.05;// Probability Of The Random Network
rp=0.001;//Rewiring Probability
//Construction of the static random network for layer-2 starts
for(i=1;i<=n;i++) for(j=1;j<=n;j++) A2[i][j]=0;
    for(i=1;i<=n;i++)
    {
      for(j=i+1;j<=n;j++)
      {
        if((float)rand()/RAND_MAX<=prand)
        {
          A2[i][j]=1;
          A2[j][i]=1;
        }
      }
    }
//Construction of the static random network for layer-2 ends
for(i3=0;i3<=10;i3++)
{
eta=6.0/100.0*i3;
for(i2=0;i2<=100;i2++)
{
eps=6.0/100.0*i2;//          printf("%d\n",i2);
avger=0.0;
for(i4=1;i4<=TT;i4++)
{
  for(i=1;i<=n;i++)
  {
    x10[i]=-7.0+0.01*(float)rand()/RAND_MAX;
    y10[i]=-10.0+0.01*(float)rand()/RAND_MAX;
    z10[i]=5.0+0.01*(float)rand()/RAND_MAX;
    x20[i]=-7.0+0.01*(float)rand()/RAND_MAX;
    y20[i]=-10.0+0.01*(float)rand()/RAND_MAX;
    z20[i]=5.0+0.01*(float)rand()/RAND_MAX;
  }
```

```
  h=0.01; w0=0.0;  er1=0.0; er2=0.0;
for(ii=1;ii<=mm;ii++)
{
//     Rewiring of the Layer-1 (Random Network) Starts
  if((((float)rand()/RAND_MAX)<=rp)||(ii==1))
  {
    for(i=1;i<=n;i++) for(j=1;j<=n;j++) A1[i][j]=0;
    for(i=1;i<=n;i++)
    {
      for(j=i+1;j<=n;j++)
      {
        if((float)rand()/RAND_MAX<=prand)
        {
          A1[i][j]=1;
          A1[j][i]=1;
        }
      }
    }
  }
//          Rewiring Of The Layer-1 (Random Network) Ends
  for(j=1;j<=n;j++)
  {
    sum1=0.0;
    for(m=1;m<=n;m++)
    sum1=sum1+ A1[j][m]*(x10[m]-x10[j]);
    l=sigma*(y10[j]-x10[j])+eps*sum1;
    k[1][6*j-5]=l*h;

    l=x10[j]*(rho-z10[j])-y10[j]+eta*(y20[j]-y10[j]);
    k[1][6*j-4]=l*h;

    l=x10[j]*y10[j]-beta*z10[j];
    k[1][6*j-3]=l*h;

    sum1=0.0;
    for(m=1;m<=n;m++)
      sum1=sum1+A2[j][m]*(x20[m]-x20[j]);
    l=sigma*(y20[j]-x20[j])+eps*sum1;
    k[1][6*j-2]=l*h;
    l=x20[j]*(rho-z20[j])-y20[j]+eta*(y10[j]-y20[j]);
    k[1][6*j-1]=l*h;
    l=x20[j]*y20[j]-beta*z20[j];
    k[1][6*j]=l*h;
  }
  for(j=1;j<=n;j++)
  {
    x1[j]=x10[j]+k[1][6*j-5]/2.0;
    y1[j]=y10[j]+k[1][6*j-4]/2.0;
    z1[j]=z10[j]+k[1][6*j-3]/2.0;
    x2[j]=x20[j]+k[1][6*j-2]/2.0;
    y2[j]=y20[j]+k[1][6*j-1]/2.0;
    z2[j]=z20[j]+k[1][6*j]/2.0;
  }        w=w0 +h/2.0;
  for(j=1;j<=n;j++)
  {
    sum1=0.0;
    for(m=1;m<=n;m++)
    sum1=sum1+A1[j][m]*(x1[m]-x1[j]);
    l=sigma*(y1[j]-x1[j])+eps*sum1;
    k[2][6*j-5]=l*h;

    l=x1[j]*(rho-z1[j])-y1[j]+eta*(y2[j]-y1[j]);
    k[2][6*j-4]=l*h;
    l=x1[j]*y1[j]-beta*z1[j];
```

```
  k[2][6*j-3]=l*h;
  sum1=0.0;
  for(m=1;m<=n;m++)
  sum1=sum1+A2[j][m]*(x2[m]-x2[j]);
  l=sigma*(y2[j]-x2[j])+eps*sum1;
  k[2][6*j-2]=l*h;
  l=x2[j]*(rho-z2[j])-y2[j]+eta*(y1[j]-y2[j]);
  k[2][6*j-1]=l*h;
  l=x2[j]*y2[j]-beta*z2[j];
  k[2][6*j]=l*h;
}
for(j=1;j<=n;j++)
{
  x1[j]=x10[j]+(k[2][6*j-5]/2.0);
  y1[j]=y10[j]+(k[2][6*j-4]/2.0);
  z1[j]=z10[j]+(k[2][6*j-3]/2.0);
  x2[j]=x20[j]+(k[2][6*j-2]/2.0);
  y2[j]=y20[j]+(k[2][6*j-1]/2.0);
  z2[j]=z20[j]+(k[2][6*j]/2.0);
}       w=w0+h/2.0;
for(j=1;j<=n;j++)
{
  sum1=0.0;
  for(m=1;m<=n;m++)
  sum1=sum1+A1[j][m]*(x1[m]-x1[j]);
  l=sigma*(y1[j]-x1[j])+eps*sum1;
  k[3][6*j-5]=l*h;
  l=x1[j]*(rho-z1[j])-y1[j]+eta*(y2[j]-y1[j]);
  k[3][6*j-4]=l*h;
  l=x1[j]*y1[j]-beta*z1[j];
  k[3][6*j-3]=l*h;
  sum1=0.0;
  for(m=1;m<=n;m++)
  sum1=sum1+A2[j][m]*(x2[m]-x2[j]);
  l=sigma*(y2[j]-x2[j])+eps*sum1;
  k[3][6*j-2]=l*h;
  l=x2[j]*(rho-z2[j])-y2[j]+eta*(y1[j]-y2[j]);
  k[3][6*j-1]=l*h;
  l=x2[j]*y2[j]-beta*z2[j];
  k[3][6*j]=l*h;
}
for(j=1;j<=n;j++)
{
  x1[j]=x10[j]+k[3][6*j-5];
  y1[j]=y10[j]+k[3][6*j-4];
  z1[j]=z10[j]+k[3][6*j-3];
  x2[j]=x20[j]+k[3][6*j-2];
  y2[j]=y20[j]+k[3][6*j-1];
  z2[j]=z20[j]+k[3][6*j];
}     w=w0+h;
for(j=1;j<=n;j++)
{
  sum1=0.0;
  for(m=1;m<=n;m++)
  sum1=sum1+A1[j][m]*(x1[m]-x1[j]);
  l=sigma*(y1[j]-x1[j])+eps*sum1;
  k[4][6*j-5]=l*h;
  l=x1[j]*(rho-z1[j])-y1[j]+eta*(y2[j]-y1[j]);
  k[4][6*j-4]=l*h;
  l=x1[j]*y1[j]-beta*z1[j];
  k[4][6*j-3]=l*h;
  sum1=0.0;
  for(m=1;m<=n;m++)
```

```
      sum1=sum1+A2[j][m]*(x2[m]-x2[j]);
      l=sigma*(y2[j]-x2[j])+eps*sum1;
      k[4][6*j-2]=l*h;
      l=x2[j]*(rho-z2[j])-y2[j]+eta*(y1[j]-y2[j]);
      k[4][6*j-1]=l*h;
      l=x2[j]*y2[j]-beta*z2[j];
      k[4][6*j]=l*h;
    }
    for(j=1;j<=n;j++)
    {
      x10[j]=x10[j]+(k[1][6*j-5]+2.0*(k[2][6*j-5]+k[3][6*j-5])+k[4][6*j-5])/6.0;
      y10[j]=y10[j]+(k[1][6*j-4]+2.0*(k[2][6*j-4]+k[3][6*j-4])+k[4][6*j-4])/6.0;
      z10[j]=z10[j]+(k[1][6*j-3]+2.0*(k[2][6*j-3]+k[3][6*j-3])+k[4][6*j-3])/6.0;
      x20[j]=x20[j]+(k[1][6*j-2]+2.0*(k[2][6*j-2]+k[3][6*j-2])+k[4][6*j-2])/6.0;
      y20[j]=y20[j]+(k[1][6*j-1]+2.0*(k[2][6*j-1]+k[3][6*j-1])+k[4][6*j-1])/6.0;
      z20[j]=z20[j]+(k[1][6*j]+2.0*(k[2][6*j]+k[3][6*j])+k[4][6*j])/6.0;
    }
    w0=w0+h;
    if(ii>tn)
    {//      fprintf(fp1,"%f",w0); for(j=1;j<=n;j++) fprintf(fp1,"\t%f\t%f",x10[j],x20[j]);
     //fprintf(fp1,"\t%f\t%f\t%f\t%f\t%f\t%f",x10[j],y10[j],z10[j],x20[j],y20[j],z20[j]);
//    fprintf(fp1,"\n");
      sum1=0.0;
      for(j=2;j<=n;j++)
      sum1=sum1+sqrt(pow(x10[j]-x10[1],2.0)+pow(y10[j]-y10[1],2.0)+pow(z10[j]-z10[1],2.0));
      er1=er1+sum1/(n-1.0);
      sum1=0.0;
      for(j=2;j<=n;j++)
      sum1=sum1+sqrt(pow(x20[j]-x20[1],2.0)+pow(y20[j]-y20[1],2.0)+pow(z20[j]-z20[1],2.0));
      er2=er2+sum1/(n-1.0);
    }
  }
    er1=er1/(mm-tn);
    er2=er2/(mm-tn);
    error=(er1+er2)/2.0;
    avger=avger+error;
  }
    printf("%f\t%f\t%f\t%f\n",eps,eta,rp,avger/TT);
    fprintf(fp2,"%f\t%f\t%f\t%f\n",eps,eta,rp,avger/TT);
  }
  }
  return 0;
  fclose(fp1);
  fclose(fp2);
  }
```

The following code for calculation of maximum Lyapunov exponent of the transverse error system with two layer multiplex network.

```
#include <stdio.h>
#include <stdlib.h>
#include <math.h>
#include <time.h>
main()
{
srand(time(NULL));
int i,j,j1,ii,n,m,mm,j2,j3,i2,i3,n1,l1,rf,rp,np,k1,IRAND,TT,k2,k3,k4,k5,nn,tn,i1;
float cum[7],v[45],gsc[7],p,temp,w0,t0,h,l,w,sigma,rho,beta,eps,eta,RAND,ev1,ev2,znorm[7],mle;
float ax10,ax1,ay10,ay1,az10,az1,ax20,ax2,ay20,ay2,az20,az2,x10,x1,y10,y1,z10,z1,x20,x2,y20,y2,z20,z2;
float k14,k15,k16,k24,k25,k26,k34,k35,k36,k44,k45,k46,k42,k43,k11,k12,k13,k21,k22,k23,k31,k32,k33,k41;
FILE *fopen(),*fp1,*fp2;
fp1=fopen("L_M_mle_old.out","w");
fp2=fopen("L_ts.out","w");
n=6; nn=n*(n+1);TT=50; p=0.05;
ev1=1.5503785424;
ev2=200.0*p;
sigma=10.0;        beta=8.0/3.0;        rho=28.0;
mm=1000000; // Time Iteration
tn=200000; // Transient Time
for(i2=0;i2<=0;i2++)
{
  eps=6.0/100.0*i2;
  printf("%d\n",i2);
  for(i3=0;i3<=0;i3++)
  {
    eta=5.0/100.0*i3;  mle=0.0;
    for(i1=1;i1<=TT;i1++)
    {
    x10=-7.0+0.01*(float)rand()/RAND_MAX;
    y10=-10.0+0.01*(float)rand()/RAND_MAX;
    z10=5.0+0.01*(float)rand()/RAND_MAX;
    x20=-7.0+0.01*(float)rand()/RAND_MAX;
    y20=-10.0+0.01*(float)rand()/RAND_MAX;
    z20=5.0+0.01*(float)rand()/RAND_MAX;
   for(i=n+1;i<=nn;i++)
      v[i]=0.0;
    for(i=1;i<=n;i++)
    {
      v[(n+1)*i]=1.0;
           cum[i]=0.0;
    }
    h=0.01; w0=0.0;
    for(ii=1;ii<=mm;ii++)
    {
      l=sigma*(y10-x10);   k11=l*h;
      l=x10*(rho-z10)-y10+eta*(y20-y10);    k12=l*h;
      l=x10*y10-beta*z10;  k13=l*h;
      l=sigma*(y20-x20);   k14=l*h;
      l=x20*(rho-z20)-y20+eta*(y10-y20);   k15=l*h;
      l=x20*y20-beta*z20;  k16=l*h;
      x1=x10+k11/2.0; y1=y10+k12/2.0; z1=z10+k13/2.0;
      x2=x20+k14/2.0; y2=y20+k15/2.0; z2=z20+k16/2.0;
      w=w0 +h/2.0;
      l=sigma*(y1-x1);  k21=l*h;
      l=x1*(rho-z1)-y1+eta*(y2-y1); k22=l*h;
      l=x1*y1-beta*z1;  k23=l*h;

      l=sigma*(y2-x2); k24=l*h;
      l=x2*(rho-z2)-y2+eta*(y1-y2); k25=l*h;
```

```
l=x2*y2-beta*z2; k26=l*h;
x1=x10+k21/2.0; y1=y10+k22/2.0; z1=z10+k23/2.0;
x2=x20+k24/2.0; y2=y20+k25/2.0; z2=z20+k26/2.0;
w=w0+h/2.0;
l=sigma*(y1-x1);  k31=l*h;
l=x1*(rho-z1)-y1+eta*(y2-y1); k32=l*h;
l=x1*y1-beta*z1; k33=l*h;
l=sigma*(y2-x2); k34=l*h;
l=x2*(rho-z2)-y2+eta*(y1-y2); k35=l*h;
l=x2*y2-beta*z2; k36=l*h;
x1=x10+k31; y1=y10+k32; z1=z10+k33;
x2=x20+k34; y2=y20+k35; z2=z20+k36;
w=w0+h;
 l=sigma*(y1-x1); k41=l*h;
l=x1*(rho-z1)-y1+eta*(y2-y1);  k42=l*h;
l=x1*y1-beta*z1; k43=l*h;
l=sigma*(y2-x2); k44=l*h;
l=x2*(rho-z2)-y2+eta*(y1-y2); k45=l*h;
l=x2*y2-beta*z2; k46=l*h;
x10=x10+(k11+2.0*(k21+k31)+k41)/6.0;
y10=y10+(k12+2.0*(k22+k32)+k42)/6.0;
z10=z10+(k13+2.0*(k23+k33)+k43)/6.0;
x20=x20+(k14+2.0*(k24+k34)+k44)/6.0;
y20=y20+(k15+2.0*(k25+k35)+k45)/6.0;
z20=z20+(k16+2.0*(k26+k36)+k46)/6.0;
w0=w0+h;
if(ii>tn)
{          fprintf(fp2,"%f\t%f\t%f\t%f\t\n",w0,x10,y10,z10);
  for(j1=0;j1<=n-1;j1++)
  {
    ax10=v[7+j1]; ay10=v[13+j1]; az10=v[19+j1];
    ax20=v[25+j1]; ay20=v[31+j1]; az20=v[37+j1];
    l=sigma*(ay10-ax10)-eps*ev1*ax10;  k11=l*h;
    l=(rho-z10)*ax10-ay10-x10*az10+eta*(ay20-ay10);  k12=l*h;
    l=y10*ax10+x10*ay10-beta*az10; k13=l*h;
    l=sigma*(ay20-ax20)-eps*ev2*ax20; k14=l*h;
    l=(rho-z20)*ax20-ay20-x20*az20+eta*(ay10-ay20); k15=l*h;
    l=y20*ax20+x20*ay20-beta*az20; k16=l*h;
    ax1=ax10+k11/2.0; ay1=ay10+k12/2.0; az1=az10+k13/2.0;
    ax2=ax20+k14/2.0; ay2=ay20+k15/2.0;az2=az20+k16/2.0;
    w=w0 +h/2.0;
    l=sigma*(ay1-ax1)-eps*ev1*ax1;k21=l*h;
    l=(rho-z10)*ax1-ay1-x10*az1+eta*(ay2-ay1);k22=l*h;
    l=y10*ax1+x10*ay1-beta*az1; k23=l*h;
    l=sigma*(ay2-ax2)-eps*ev2*ax2; k24=l*h;
    l=(rho-z20)*ax2-ay2-x20*az2+eta*(ay1-ay2); k25=l*h;
    l=y20*ax2+x20*ay2-beta*az2; k26=l*h;
    ax1=ax10+k21/2.0;ay1=ay10+k22/2.0;az1=az10+k23/2.0;
    ax2=ax20+k24/2.0; ay2=ay20+k25/2.0;az2=az20+k26/2.0;
    w=w0+h/2.0;
    l=sigma*(ay1-ax1)-eps*ev1*ax1;k31=l*h;
    l=(rho-z10)*ax1-ay1-x10*az1+eta*(ay2-ay1); k32=l*h;
    l=y10*ax1+x10*ay1-beta*az1; k33=l*h;
    l=sigma*(ay2-ax2)-eps*ev2*ax2; k34=l*h;
    l=(rho-z20)*ax2-ay2-x20*az2+eta*(ay1-ay2); k35=l*h;
    l=y20*ax2+x20*ay2-beta*az2; k36=l*h;
    ax1=ax10+k31;ay1=ay10+k32;az1=az10+k33;
    ax2=ax20+k34;ay2=ay20+k35;az2=az20+k36;
    w=w0+h;
    l=sigma*(ay1-ax1)-eps*ev1*ax1; k41=l*h;

    l=(rho-z10)*ax1-ay1-x10*az1+eta*(ay2-ay1); k42=l*h;
    l=y10*ax1+x10*ay1-beta*az1; k43=l*h;
```

```
            l=sigma*(ay2-ax2)-eps*ev2*ax2; k44=l*h;
            l=(rho-z20)*ax2-ay2-x20*az2+eta*(ay1-ay2); k45=l*h;
            l=y20*ax2+x20*ay2-beta*az2; k46=l*h;
            ax10=ax10+(k11+2.0*(k21+k31)+k41)/6.0;
            ay10=ay10+(k12+2.0*(k22+k32)+k42)/6.0;
            az10=az10+(k13+2.0*(k23+k33)+k43)/6.0;
            ax20=ax20+(k14+2.0*(k24+k34)+k44)/6.0;
            ay20=ay20+(k15+2.0*(k25+k35)+k45)/6.0;
            az20=az20+(k16+2.0*(k26+k36)+k46)/6.0;
             w0=w0+h;
            v[7+j1]=ax10; v[13+j1]=ay10; v[19+j1]=az10;
            v[25+j1]=ax20; v[31+j1]=ay20;v[37+j1]=az20;
          }
          znorm[1]=0.0;
          for(j=1;j<=n;j++)
            znorm[1]=znorm[1]+pow(v[n*j+1],2.0);
          znorm[1]=sqrt(znorm[1]);
               for(j=1;j<=n;j++)
                 v[n*j+1]=v[n*j+1]/znorm[1];
          for(j=2;j<=n;j++)
          {
                for(k1=1;k1<=j-1;k1++)
            {
                  gsc[k1]=0.0;
                  for(l1=1;l1<=n;l1++)
                    gsc[k1]=gsc[k1]+v[n*l1+j]*v[n*l1+k1];
            }
            for(k2=1;k2<=n;k2++)
            {
                  for(l1=1;l1<=j-1;l1++)
                    v[n*k2+j]=v[n*k2+j]-gsc[l1]*v[n*k2+l1];
            }
            znorm[j]=0.0;
                 for(k3=1;k3<=n;k3++)
            znorm[j]=znorm[j]+pow(v[n*k3+j],2.0);
            znorm[j]=sqrt(znorm[j]);
             for(k4=1;k4<=n;k4++)
            v[n*k4+j]=v[n*k4+j]/znorm[j];
          }
            for(k5=1;k5<=n;k5++)
           cum[k5]=cum[k5]+log(znorm[k5])/log(2.0);
        }
        w0=w0+h;
      }//    Time Iteration (ii)
      t0=w0-tn*h;
      for(i=1;i<=n;i++)
      {
        for(j=i+1;j<=n;j++)
        {
          if(cum[j]>cum[i])
          {
            temp=cum[i];  cum[i]=cum[j]; cum[j]=temp;
          }
        }
      }
        mle=mle+cum[1]/t0;//printf("%f\n",cum[1]/t0);
      }
      fprintf(fp1,"%f\t%f\t%f\n",eps,eta,mle/TT);
    }
  }
return 0;
fclose(fp1);fclose(fp2);
}
```